ABSTRACT

Title of dissertation: ASYMMETRIC FLUID CRITICALITY

Christopher Elliot Bertrand,
Doctor of Philosophy, 2011

Dissertation directed by: Professor Mikhail Anisimov,
Institute for Physical Science and Technology &
Department of Chemical and Biomolecular Engineering

This work investigates features of critical phenomena in fluids. The canonical description of critical phenomena, inspired by the Ising model, fails to capture all features observed in fluid systems, specifically those associated with the density or compositional asymmetry of phase coexistence. A new theory of fluid criticality, known as "complete scaling", was recently introduced. Given its success in describing experimental results, complete scaling appears to supersede the previous theory of fluid criticality that was consistent with a renormalization group (RG) analysis of an asymmetric Landau-Ginzburg-Wilson (LGW) Hamiltonian. In this work, the complete scaling approach and the equation of state resulting from the RG analysis are shown to be consistent to order ϵ, where $\epsilon = 4 - d$ with d being the spatial dimensionality. This is accomplished by developing a complete scaling equation of state, and then defining a mapping between the complete scaling mixing-parameters and the coefficients of the asymmetric LGW Hamiltonian, thereby generalizing previous work [Phys. Rev. Lett. **97**, 025703 (2006)] on mean-field equations of state.

The seemingly different predictions of these approaches are shown to stem from an intrinsic ambiguity in the interpretation of the ϵ-expansion at fixed order. To first order in ϵ it is found that the asymmetric correction-to-scaling exponent θ_5 predicted by the RG calculations can be fully absorbed into the 2β exponent of complete scaling.

Complete scaling is then extended to spatially inhomogeneous fluids in the approximation $\eta = 0$, where η is the anomalous dimension. This extension enables one to obtain a fluctuation-modified asymmetric interfacial density profile, which incorporates effects from both the asymmetry of fluid phase coexistence and the associated asymmetry of the correlation length. The derived asymmetric interfacial profile is used to calculate Tolman's length, the coefficient of the first curvature correction to the surface tension. The previously predicted divergence of Tolman's length at the critical point is confirmed and the amplitude of this divergence is found to depend nonuniversally on the asymmetry of the correlation length.

ASYMMETRIC FLUID CRITICALITY

by

Christopher Elliot Bertrand

Dissertation submitted to the Faculty of the Graduate School of the
University of Maryland, College Park in partial fulfillment
of the requirements for the degree of
Doctor of Philosophy
2011

Advisory Committee:
Professor Mikhail A. Anisimov, Chair
Professor Michael E. Fisher
Professor Michelle Girvan
Professor Christopher Jarzynski, Dean's representative
Professor Jan V. Sengers
Professor John D. Weeks

© Copyright by
Christopher Elliot Bertrand
2011

Acknowledgments

Acknowledgement is made to the donors of the ACS Petroleum Research Fund for support of this research.

I am indebted to a several people to who have helped me get to this point: My advisor, Mikhail Anisimov, for being a patient and dedicated mentor. Your enthusiasm for science and life is inspiring. I have benefited greatly from your advice, instruction and advocacy. Thank you. Jan Sengers, for providing additional expertise, perspective, and encouragement. My friends in the physics department, Jordan Horowitz, Jonah Kanner, and Ryan Behunin, who have helped me navigate through classes, the administrative bureaucracy, and life over the last five years. Deepa Subramanian, for her cheerful company around the office. And finally, my parents, Kathleen Postle and Kevin Bertrand, for their support and unflagging confidence in my potential.

Table of Contents

List of Tables v

List of Figures vi

List of Abbreviations and Symbols vii

1 Introduction 1
- 1.1 Overview . . . 1
- 1.2 Fluid Criticality . . . 2
  - 1.2.1 Asymptotic critical phenomena . . . 4
  - 1.2.2 Universality and corrections to scaling . . . 9
  - 1.2.3 Fluid asymmetry . . . 12
- 1.3 Mean-field equations of state . . . 16
  - 1.3.1 Ising model/Lattice Gas . . . 17
  - 1.3.2 Asymmetric Landau expansion . . . 19
  - 1.3.3 Complete scaling in mean-field approximation . . . 21

2 Complete scaling and the renormalization group 23
- 2.1 Introduction . . . 23
- 2.2 Complete scaling equation of state . . . 25
  - 2.2.1 Equation of state for the Helmholtz energy . . . 29
  - 2.2.2 Linear model . . . 31
  - 2.2.3 ϵ-expansion . . . 31
- 2.3 RG treatment of fluid asymmetry . . . 36
- 2.4 Consistency of complete scaling at $O(\epsilon)$ . . . 41
- 2.5 Comparison with experiment . . . 48
- 2.6 Summary and Conclusions . . . 51

3 Complete scaling for inhomogeneous fluids 55
- 3.1 Introduction . . . 55
- 3.2 Thermodynamics of non-uniform systems . . . 61
- 3.3 Complete scaling for inhomogeneous fluids . . . 64
  - 3.3.1 Equilibrium conditions . . . 69
- 3.4 Asymmetric profile ($b = 0$) . . . 72
- 3.5 Interfacial entropy profile . . . 76
  - 3.5.1 Full interfacial density profile . . . 78
  - 3.5.2 Interfacial heat capacity . . . 80
- 3.6 Tolman's length . . . 82
- 3.7 Summary and Conclusions . . . 85

4 Summary and Discussion 86

A Ising-type equation of state in the one-loop approximation 91

Bibliography 99

List of Tables

1.1 Critical exponents for 3D Ising model 10
1.2 Mean-field critical exponents 19
1.3 Mean-field critical amplitudes 19

2.1 Critical parameters and amplitudes 52
2.2 Mixing parameters and asymmetry coefficients 53

3.1 Estimates of Tolman's length amplitude δ_0 84

A.1 Critical exponents in the one-loop approximation at $O(\epsilon)$ 97
A.2 Critical amplitudes in the one-loop approximation at $O(\epsilon)$ based on the Ising-type EOS Eq. A.24 98

List of Figures

1.1 Coexistence curve of SF_6 in the P-T plane 3
1.2 Coexistence curve of SF_6 in the ρ-T plane 4
1.3 Isochoric heat-capacity of SF_6 6
1.4 Symmetric Ising/lattice-gas coexistence curve 11
1.5 Excess density of SF_6 near the critical point 13
1.6 Schematic asymmetric mean-field coexistence curve 21

2.1 Asymmetric vertex-function diagrams up to one loop 38
2.2 Comparison of experimental and theoretical liquid-vapor excess densities 49
2.3 Complete scaling mixing-parameters and asymmetry coefficients . . . 50

3.1 Symmetric interfacial profiles 57
3.2 Interfacial profile functions 73

A.1 Ising vertex-function diagrams up to one loop 93

List of Abbreviations and Symbols

Abbrv.	
EOS	equation of state
LGW	Landau-Ginzburg-Wilson
$O(\epsilon)$	order ϵ
RG	renormalization group
Greek	
α	heat-capacity exponent
β	magnetization exponent
γ	susceptibility exponent
$\Gamma_0^{\pm}$	magnetic-susceptibility amplitude
δ	magnetic-field exponent
δ_{T}	Tolman's length
Δ	symmetric correction-to-scaling exponent
ϵ	$4-d$
η	the anomalous dimension
θ_5	asymmetric correction-to-scaling exponent
κ^2	$t+(g/2)m^2$
κ_T	isothermal compressibility
μ, $\hat{\mu}$, $\Delta\mu$	chemical potential, $\mu/k_{\mathrm{B}}T_{\mathrm{c}}$, $\hat{\mu}-\hat{\mu_c}$
ν	correlation-length exponent
ξ	correlation length
$\xi_0^{\pm}$	correlation-length amplitude
ρ, $\hat{\rho}$, $\Delta\rho$	density, ρ/ρ_{c}, $\hat{\rho}-1$
ρ_{liq}, ρ_{vap}	density of the liquid and vapor phases
$\Delta\rho^+$, $\Delta\rho^-$	$\hat{\rho}_{\mathrm{liq}}-1$, $\hat{\rho}_{\mathrm{vap}}-1$
$\Delta\rho_0$	$(\Delta\rho^+-\Delta\rho^-)/2$; "density difference"
$\overline{\Delta\rho}$	$(\Delta\rho^++\Delta\rho^-)/2$; "excess density"
σ	surface tension
Σ	interfacial surface-area
ϕ	order-parameter field
Φ	Ising grand-potential
χ	magnetic susceptibility
χ_T	isothermal susceptibility
Ψ	Ising Helmholtz-energy density
Latin	
a	pressure-mixing constant
$\hat{a}$	$a(1+\epsilon/12)$
$A_0^{\pm}$	heat-capacity amplitude
b	chemical-potential mixing constant
B_0	magnetization amplitude
B_1	amplitude of magnetization Wegner-correction
B_{cr}	critical heat-capacity background

Latin

c	non-linear mixing constant
$\hat{c}$	gc
C_ρ	isochoric heat-capacity per molecule
d	number of spatial dimensions
f, $\hat{f}$, Δf	Helmholtz-energy density, $f/\rho_{\rm c}k_{\rm B}T_{\rm c}$, $\hat{f}-\hat{f}_{\rm c}$
f_i	Landau-expansion coefficients
g	Ising coupling constant
h	magnetic field
$\mathcal{H}$	Hamiltonian density
I	interfacial-profile function
$k_{\rm B}$	Boltzmann's constant
L	$\ln\kappa^2$
m	magnetization
M	magnetization-profile function
P, $\hat{P}$, ΔP	pressure, $P/\rho_{\rm c}k_{\rm B}T_{\rm c}$, $\hat{P}-\hat{P}_{\rm c}$
q	wave number
R	radius of curvature
s, $\hat{s}$, Δs	entropy density, $s/\rho_{\rm c}k_{\rm B}$, $\hat{s}-\hat{s_{\rm c}}$
S	entropy-profile function
t	reduced temperature in the Ising system
T, $\hat{T}$, ΔT	temperature, $T/T_{\rm c}$, $\hat{T}-1$
u_i	normalized mean-field asymmetry coefficients
$\mathbf{w}$	thermodynamic field conjugate to $\nabla\rho$
Z	partition function

Subscripts

c	evaluated at the critical point
cxc	taken along the coexistence curve

Chapter 1

Introduction

1.1 Overview

Critical phenomena are observed in a variety of diverse systems such as ferromagnets, liquid crystals, liquid-vapor systems and liquid mixtures [1]. The basic features of critical phenomena, the most striking of which are singularities in various equilibrium and transport properties, have been known for some time [2, 3, 4], and the highly successful modern theory of critical phenomena [5], based on the renormalization group (RG) [6, 7], is by this point also quite mature. However, some fundamental issues concerning critical phenomena in fluids have yet to be resolved.

Critical phenomena in liquid-vapor systems and liquid mixtures require special consideration [8, 9]. Throughout this work, we will focus on liquid-vapor systems for concreteness. This does not limit the broader implications of our discussion, since liquid mixtures are connected to liquid-vapor systems via the isomorphism principle [10, 11, 12], so that one may still generally speak of fluid criticality. The leading asymptotic behavior of fluids is known to be well-described by the Ising model [13]. However, the sub-leading terms exhibit asymmetries not present in the Ising model. Prior to the advent of RG techniques, the asymmetric features of fluid criticality were described by a phenomenological theory known as revised scaling [14, 15], which was based on the behavior of exactly soluble models [16, 17, 18, 19]. The subsequent

RG based theory of asymmetric fluid criticality confirmed the validity of revised scaling and introduced a new higher-order asymmetric correction characterized by an exponent θ_5 [20, 21, 22, 23, 24]. Relatively recently, it has been argued that a generalization of revised scaling [14], known as "complete scaling", is necessary for the accurate description of asymmetric fluid criticality [25, 26]. Complete scaling predicts a new leading-order asymmetric correction term and has been successfully used to describe experimental results [27, 28, 29].

This work investigates the foundations of complete scaling, and a particular extension of complete scaling. In this chapter, an introduction to critical phenomena in fluids is presented. Section 1.2 starts with general concepts, which are then applied to the mean-field equation of state in Sec. 1.3. The material in this chapter provides sufficient background for understanding the results presented in Chapters 2 and 3. In Chapter 2, the predictions of complete scaling and the RG treatment of asymmetry are compared, and the two approaches are shown to be equivalent at $O(\epsilon)$ in the ϵ-expansion, $\epsilon = 4 - d$, where d is the spatial dimensionality. An extension of complete scaling to inhomogeneous systems, which allows for the calculation of Tolman's length, is presented in Chapter 3. The implications of the these results and future research directions are discussed in Chapter 4

1.2 Fluid Criticality

Figure 1.1 shows the phase diagram of sulfur hexafluoride (SF_6) in the P-T plane, where P is pressure, and T is temperature. The coexistence curve which

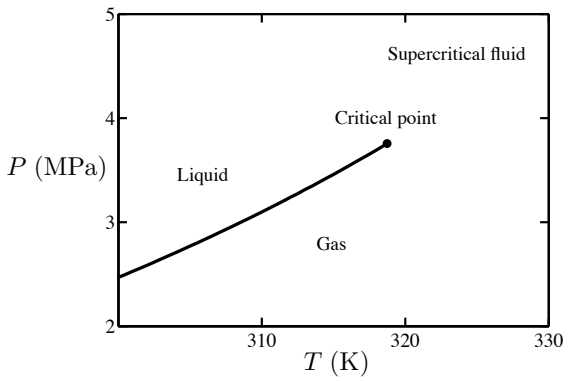

Figure 1.1: Schematic coexistence curve of SF_6 in the P-T plane.

separates the liquid and gas phases is terminated by a critical point located at the critical pressure and temperature, $P_c = 3.76$ MPa and $T_c = 318.7$ K. Above the critical point, there is only a single supercritical fluid phase. Along the coexistence curve, distinct liquid and vapor phases coexist in equilibrium. To better illustrate the nature of the liquid-vapor equilibrium, the coexistence curve is presented in Fig. 1.2 in the ρ-T plane, where ρ is density. For densities and temperatures inside the coexistence curve, the system separates into a liquid phase and a vapor phase. The densities of these phases, which define the two branches of the coexistence curve, are given by $\rho_{\rm liq}(T)$ and $\rho_{\rm vap}(T)$. As the critical point is approached, the density difference $\rho_{\rm liq} - \rho_{\rm vap}$ vanishes and certain thermodynamic properties exhibit singular behavior.

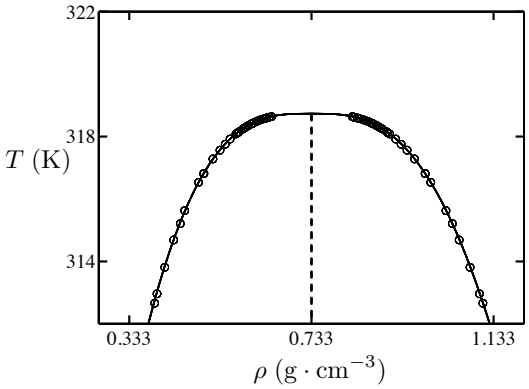

Figure 1.2: ρ-T diagram of the SF_6 coexistence curve. Open circles correspond to experimental data [30, 31]. The dashed line is the critical isochore

1.2.1 Asymptotic critical phenomena

For the description of phenomena in the vicinity of the critical point, it is convenient to utilize dimensionless variables defined by

$$\hat{T} = \frac{T}{T_\mathrm{c}}, \quad \hat{\rho} = \frac{\rho}{\rho_\mathrm{c}}, \quad \hat{P} = \frac{P}{\rho_\mathrm{c} k_\mathrm{B} T_\mathrm{c}}, \tag{1.1}$$

and, for future reference,

$$\hat{\mu} = \frac{\mu}{k_\mathrm{B} T_\mathrm{c}}, \quad \hat{s} = \frac{s}{\rho_\mathrm{c} k_\mathrm{B}}, \quad \hat{f} = \frac{f}{\rho_\mathrm{c} k_\mathrm{B} T_\mathrm{c}}, \tag{1.2}$$

where we have introduced the chemical potential μ, the entropy density s, and the Helmholtz free energy density f, or the Helmholtz energy for short. Here, k_B is Boltzmann's constant. The reference point of the thermodynamic coordinate system can be shifted to the critical point by defining reduced variables as

$$\begin{aligned} \Delta T &= \frac{T - T_\mathrm{c}}{T_\mathrm{c}}, \quad \Delta\rho = \frac{\rho - \rho_\mathrm{c}}{\rho_\mathrm{c}}, \quad \Delta P = \frac{P - P_\mathrm{c}}{\rho_\mathrm{c} k_\mathrm{B} T_\mathrm{c}}, \\ \Delta\mu &= \frac{\mu - \mu_\mathrm{c}}{k_\mathrm{B} T_\mathrm{c}}, \quad \Delta s = \frac{s - s_\mathrm{c}}{\rho_\mathrm{c} k_\mathrm{B}}, \quad \Delta f = \frac{f - f_\mathrm{c}}{\rho_\mathrm{c} k_\mathrm{B} T_\mathrm{c}}. \end{aligned} \tag{1.3}$$

The reduced liquid density is denoted by $\Delta\rho^+ = (\rho_{\rm liq} - \rho_{\rm c})/\rho_{\rm c}$ and the reduced vapor density by $\Delta\rho^- = (\rho_{\rm vap} - \rho_{\rm c})/\rho_{\rm c}$.

Near the critical point, the behavior of the system is found to be described by power laws. Along the critical isochore ($\rho = \rho_{\rm c}$), the density and the entropy density behave as

$$\Delta\rho^{\pm} \approx \begin{cases} 0 & \Delta T > 0 \\ \pm B_0 |\Delta T|^{\beta} & \Delta T < 0 \end{cases} \tag{1.4}$$

where $\pm$ corresponds to the liquid and vapor branches of the coexistence curve, and

$$\Delta s \approx \frac{A_0^{\pm}}{1-\alpha} \Delta T |\Delta T|^{-\alpha} - B_{\rm cr} \Delta T, \tag{1.5}$$

where A_0^+ and A_0^- are the heat-capacity amplitudes above and below the critical point respectively, and $B_{\rm cr}\Delta T$ is the fluctuation-induced background entropy. Here, and throughout, "$\approx$" means "asymptotically equal to". The derivatives of the densities are given by

$$\hat{\rho}\frac{\hat{C}_\rho}{\hat{T}} = \left(\frac{\partial \hat{s}}{\partial \hat{T}}\right)_\rho \approx A_0^{\pm} |\Delta T|^{-\alpha} - B_{\rm cr}, \tag{1.6}$$

and

$$\chi_T = \left(\frac{\partial \hat{\rho}}{\partial \hat{\mu}}\right)_T \approx \Gamma_0^{\pm} |\Delta T|^{-\gamma}, \tag{1.7}$$

where $\hat{C}_\rho = C_\rho / k_{\rm B}$ and C_ρ is the isochoric heat capacity per molecule and the isothermal susceptibility χ_T is related to the more common isothermal compressibility κ_T by $\chi_T = \hat{\rho}^2 \hat{\kappa}_T$. The isochoric heat capacity diverges weakly at the critical point and the isothermal susceptibility diverges strongly. Isochoric heat-capacity data for SF_6 are plotted in Fig. 1.3. The amplitude of the heat capacity is clearly different above and below the critical point. Long range fluctuations are responsible for the

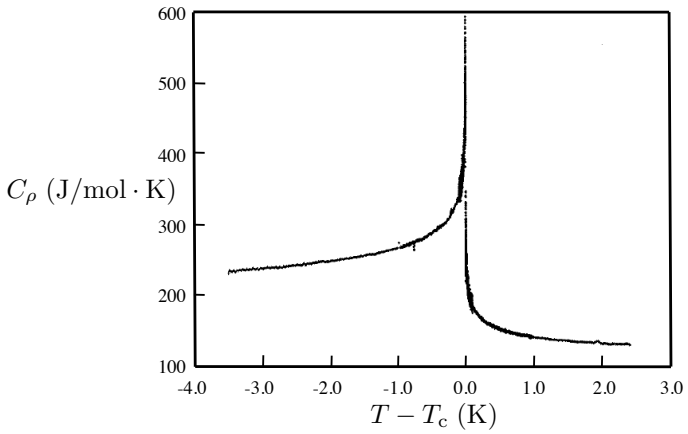

Figure 1.3: C_ρ data for SF_6 taken in microgravity on the German spacelab mission [32]. This particular data set contains roughly 2500 data points.

singular nature of the isochoric heat capacity in the critical region. The range of these fluctuations is characterized by the density-density correlation function,

$$\langle \Delta\rho(x)\Delta\rho(0)\rangle \sim \exp\frac{-x}{\xi}, \qquad x \to \infty, \tag{1.8}$$

where ξ is the correlation length, which diverges at the critical point, and is asymptotically described by,

$$\xi \approx \xi_0^{\pm}|\Delta T|^{-\nu}. \tag{1.9}$$

As the critical point is approached, the wavenumber dependence of the Fourier transform of the correlation function is also described by a power law,

$$\int \mathrm{d}x\, e^{iqx}\, \langle \Delta\rho(x)\Delta\rho(0)\rangle \sim \frac{1}{q^{2-\eta}}, \qquad \Delta T \to 0. \tag{1.10}$$

The exponent η is referred to as the anomalous dimension. Lastly, along the critical isotherm ($T = T_c$), the chemical potential varies with density as

$$\Delta\mu \sim \Delta\rho|\rho|^{\delta-1}. \tag{1.11}$$

In the above equations, the powers α, β, γ, ν, η, and δ are called critical exponents and the coefficients $A_0^{\pm}$, B_0, $\Gamma_0^{\pm}$, and $\xi_0^{\pm}$ are called critical amplitudes. As defined, the exponents and amplitudes are all positive in accordance with experimentally verified theory. The critical exponents are linked by the so-called scaling relations

$$\alpha + 2\beta + \gamma = 2, \qquad \beta(\delta - 1) = \gamma, \tag{1.12}$$

$$\gamma = \nu(2 - \eta), \qquad \alpha = 2 - \nu d, \tag{1.13}$$

where d is the dimensionality of the system, and where the final "hyperscaling" relationship is only valid for $d \leq 4$. Thus, knowledge of any two exponents is sufficient to determine the others.

The connection between the various thermodynamic variables is given by the Gibbs-Duhem relation,

$$d\hat{P} = \hat{\rho} d\hat{\mu} + \hat{s} d\hat{T}. \tag{1.14}$$

The densities are

$$\hat{\rho} = \left(\frac{\partial \hat{P}}{\partial \hat{\mu}}\right)_T, \quad \hat{s} = \left(\frac{\partial \hat{P}}{\partial \hat{T}}\right)_\mu, \tag{1.15}$$

and the susceptibilities are

$$\left(\frac{\partial \hat{\rho}}{\partial \hat{\mu}}\right)_T = \left(\frac{\partial^2 \hat{P}}{\partial \mu^2}\right)_T, \quad \left(\frac{\partial \hat{s}}{\partial \hat{T}}\right)_\mu = \left(\frac{\partial^2 \hat{P}}{\partial \hat{T}^2}\right)_\mu. \tag{1.16}$$

All of these properties are related to derivatives of the pressure. The asymptotic critical behavior can therefore be derived from a single equation of state (EOS) [33, 34, 35]. To leading order, the EOS based on scaling theory may be expressed as,

$$\Delta P \approx |\Delta T|^{2-\alpha} X^{\pm}\left(\frac{\Delta \mu}{|\Delta T|^{\beta+\gamma}}\right) + \hat{P}_{\mathrm{r}}(\mu, T), \tag{1.17}$$

where the function $X^{\pm}$ is different above and below the critical point, and where $\hat{P}_{\rm r}(\mu, T)$ is the regular, *i.e.* analytic, part of the pressure. In this form, Eq. 1.17, is known as the scaling EOS, and $\Delta\mu$ and ΔT are known as scaling fields. The term field arises from the convention that P, μ, and T are called thermodynamic fields since their conjugate variables are called densities [10].

The pressure may be regarded as a function of chemical potential and temperature. However, it is often easier to consider the density and the temperature as the independent variables. The Helmholtz energy is naturally considered a function of these two variables, and is related to the pressure by a Legendre transformation,

$$\hat{f} = \hat{P} - \hat{\mu}\hat{\rho}. \tag{1.18}$$

The differential of $\hat{f}$ is

$$d\hat{f} = \hat{\mu} d\hat{\rho} - \hat{s} d\hat{T}, \tag{1.19}$$

from which we find

$$\hat{\mu} = \left(\frac{\partial \hat{f}}{\partial \hat{\rho}}\right)_T, \quad \hat{s} = -\left(\frac{\partial \hat{f}}{\partial \hat{T}}\right)_\rho, \tag{1.20}$$

and

$$\chi_T^{-1} = \left(\frac{\partial \hat{\mu}}{\partial \hat{\rho}}\right)_T, \quad \hat{\rho}\frac{\hat{C}_\rho}{\hat{T}} = \left(\frac{\partial \hat{s}}{\partial \hat{T}}\right)_\rho. \tag{1.21}$$

Again, all asymptotic critical behavior can be derived from a scaling EOS for the Helmholtz energy,

$$\Delta\hat{f} \approx |\Delta T|^{2-\alpha} Y^{\pm}\left(\frac{\Delta\rho}{|\Delta T|^{\beta}}\right) + \hat{f}_{\rm r}(\rho, T), \tag{1.22}$$

where $\hat{f}_{\rm r}(\rho, T)$ is regular part of the Helmholtz density.

1.2.2 Universality and corrections to scaling

Critical phenomena exhibit a striking degree of universality. All critical behavior can be grouped into universality classes [1]. The members of a particular class are described by the same critical exponents. The critical behavior of uniaxial magnets, liquid-vapor systems, and liquid mixtures belong to the universality class of the Ising model. The Ising model was introduced to describe uniaxial magnets, which develop a spontaneous magnetization m below the critical point (Curie point). When reformulated for the liquid-vapor transition, the Ising model is known as the lattice-gas model [36]. In order to make the connection between these models explicit, it is convienient to introduce an additional set of variables for the Ising model by defining h, t, and $-\Phi$ as the applied magnetic field, reduced temperature, and density of the "Ising" grand potential, respectively. The later is assumed to be a known function of h and t. The mapping between the Ising model and the lattice-gas can now be expressed as

$$\begin{aligned} h &= \Delta\mu, \\ t &= \Delta T, \\ \Phi &= \Delta\tilde{P}, \end{aligned} \tag{1.23}$$

where the critical part of the pressure is defined by

$$\Delta\tilde{P} = \Delta P - \hat{P}_{\mathrm{r}}(\mu, T). \tag{1.24}$$

The regular part of the pressure can be expanded as $\hat{P}_{\mathrm{r}}(\mu, T) \simeq \Delta\mu + \hat{s}_{\mathrm{c}}\Delta T + \hat{P}_{\mathrm{r}}^{(2)}(\Delta T)^2 + \cdots$. Given the Gibbs-Duhem relation $d\Phi = mdh + sdt$ it can be shown

Exponent:	β	α	γ	ν	η	δ
Value:	0.326	0.110	1.24	0.630	0.033	4.80

Table 1.1: Critical exponents for 3D Ising model

that $m = \Delta\rho$. The Ising Helmholtz energy Ψ is related to the grand potential by $\Phi = hm - \Psi$. The relationship between the Helmholtz energy in the Ising model and the lattice-gas is similarly found to be $\Psi(m,t) = \Delta\tilde{f}(\Delta\rho, \Delta T)$, where the critical part of the Helmholtz energy is defined by

$$\Delta\tilde{f} = \Delta f - \hat{f}_{\rm r}(\rho, T) \tag{1.25}$$

and where the regular part of f can be expanded as $\hat{f}_{\rm r}(\rho,T) \simeq \hat{\mu}_{\rm c}\Delta\rho - \hat{s}_{\rm c}\Delta T - \hat{f}_{\rm r}^{(2)}(\Delta T)^2 + \cdots$. Throughout the text we will make reference to the Ising magnetic variables when describing liquid-vapor systems, with the understanding that they are fully isomorphic to the lattice-gas variables. In particular, for the remainder of the text, the term "magnetization" can be taken to mean "reduced lattice-gas density".

The critical behavior of the Ising model has been the subject of extensive theoretical investigation [37], and the critical exponents have been calculated using a variety of techniques including series expansions, renormalization group (RG) approaches and Monte Carlo simulations [38]. The results are presented in Table 1.1 . Even though the critical amplitudes are system dependent *i.e.* non-universal, their ratios form universal quantities, which have also been calculated, with $A_0^+/A_0^- \simeq 0.523$, $\Gamma_0^+/\Gamma_0^- \simeq 4.8$, and $\alpha\Gamma_0^+A_0^+/(B_0)^2 \simeq 0.0581$ [39]. These predicted values have

been confirmed for fluid systems [9].

Yet, even though the liquid-vapor system and uniaxial magnets belong to the same universality class, the coexistence curve of the Ising model, as presented in Fig. 1.4, differs from that of SF_6 in Fig. 1.2. In the latter, the distance between the isochore and liquid branch of the coexistence curve is slightly greater than that between isochore and the vapor branch. This difference is manifested in the corrections to leading asymptotic behavior. In practice, the asymptotic powers laws are found to be valid for $\Delta T \lesssim 10^{-3}$. To describe critical phenomena over a larger temperature range, correction terms are needed. For the Ising model, the nature of these corrections is restricted by symmetry considerations. The energy of the Ising model is independent of the direction of the magnetization m which plays the same role as $\Delta\rho$ in fluids. Therefore, the phase diagram in Fig. 1.4 is invariant under the transformation $m \to -m$ (or $\Delta\rho \to -\Delta\rho$). Systems with this property are said to be symmetric. The leading symmetric correction terms for the magnetization are

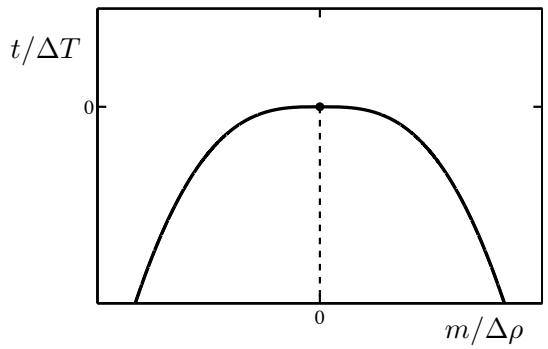

Figure 1.4: Schematic of the Ising/lattice-gas coexistence curve

given by the Wegner expansion [40], for example,

$$m^{\pm} \approx \pm B_0 |\Delta T|^{\beta} \left[1 + B_1 |\Delta T|^{\Delta}\right], \tag{1.26}$$

where the leading correction-to-scaling exponent $\Delta \simeq 0.5$ and the correction-to-scaling amplitude B_1 have been introduced. Similar expressions exist for other thermodynamic properties, like the susceptibilities. Real fluid systems, as opposed to the lattice-gas, are not subject to the Ising symmetry restriction, and are consequently expected and observed to be asymmetric. Below the critical point, any fluid property can be divided into symmetric and asymmetric parts. For instance, the symmetric portion of the fluid density, which is equivalent to the magnitude of the "magnetization", is given by the reduced density difference

$$\Delta\rho_0 = (\Delta\rho^+ - \Delta\rho^-)/2 \tag{1.27}$$

and the asymmetric portion is given by

$$\overline{\Delta\rho} = (\Delta\rho^+ + \Delta\rho^-)/2. \tag{1.28}$$

For the lattice gas, $\overline{\Delta\rho} = 0$. Consequently, we will refer to $\overline{\Delta\rho}$, when not vanishing, as the "excess density". Unlike the lattice gas, real fluids have both symmetric and asymmetric corrections to scaling.

1.2.3 Fluid asymmetry

The behavior of the excess density is of principal interest in fluid critical phenomena. The classical theory of fluid criticality predicts that $\overline{\Delta\rho} = D|\Delta T|$. This is known as the law of rectilinear diameter [41, 42], and the constant of proportionality

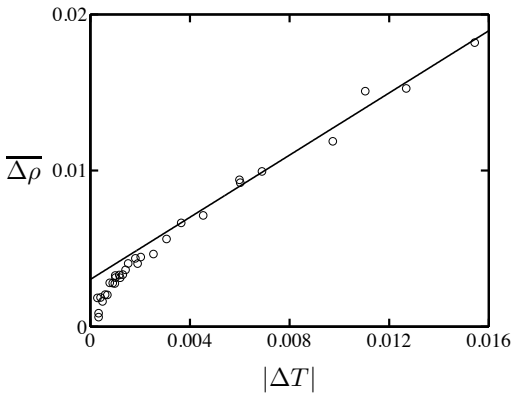

Figure 1.5: Excess density of SF_6 near the critical point [30, 31]. The data clearly show deviations from the law of rectilinear diameter near the critical point.

D is the slope of the diameter. However, as seen from the excess density data in Fig. 1.5, some fluids exhibit deviations from the predicted linearity near the critical point. Several theoretical approaches have been adopted to explain the curvature of the diameter near the critical point.

Prior to the advent of RG techniques, the dominant theory of asymmetric criticality came from a phenomenological field-mixing approach known as revised scaling [17, 18, 19, 16]. Revised scaling, which was initially based on the behavior of exactly soluble models, postulates that the physical scaling fields are linear combinations of the theoretical Ising scaling fields *i.e* $\mu(h,t)$ and $T(h,t)$. After expanding the physical fields to leading order in the symmetric fields, we can compactly express revised scaling through the following set of transformations,

$$\begin{aligned} h &= \Delta\mu, \\ t &= \Delta T + b\Delta\mu, \\ \Phi &= \Delta\tilde{P}, \end{aligned} \tag{1.29}$$

where b is phenomenological constant referred to as a mixing parameter. When combined with the Gibbs-Duhem relation for the symmetric system, $d\Phi = mdh + sdt$, this equation predicts a contribution to the excess density which varies like

$$\overline{\Delta\rho} \sim b|\Delta T|^{1-\alpha}, \tag{1.30}$$

where $1 - \alpha \simeq 0.89$. The slope of the diameter can be defined by the derivative $D = \partial\overline{\Delta\rho}/\partial|\Delta T|$. For this reason, the "$1 - \alpha$" contribution to the excess density is said to produce a "singular diameter", $D \sim |\Delta T|^{-\alpha}$.

Asymmetric fluid criticality has also been investigated using RG techniques, with two principle findings [20, 21, 22, 23, 24]. First, the validity of revised scaling was confirmed by Nicoll [24]. Second, there is an additional *asymmetric* correction-to-scaling exponent, θ_5 (also referred to as Δ_5 or $\omega_5\nu$) which creates another non-analytic contribution to the excess density

$$\overline{\Delta\rho} \sim D_{1-\alpha}|\Delta T|^{1-\alpha} + D_1|\Delta T| + D_{\theta_5}|\Delta T|^{\beta+\theta_5}, \tag{1.31}$$

where the amplitudes D_i are constant. The value of this new exponent was calculated to be $\theta_5 = 1.5$ in the first order ϵ-expansion, $\epsilon = 4 - d$ [20, 21, 22], but this expansion does not converge well as higher orders in ϵ are included [23, 43]. All estimates of θ_5 are consistent with $\beta + \theta_5 \gtrsim 1.3$ [43]. Therefore, the $\beta + \theta_5$ term appears to be of significantly higher order than the linear contribution to $\overline{\Delta\rho}$ and is thus not expected to contribute to the leading deviations from linearity near the critical point. The combination of the θ_5 term and the $1 - \alpha$ term fail to accurately describe highly asymmetric fluids and imply a non-monotonic "wiggle" in the diameter which cannot be detected in real experiments [28, 29].

Recently, Fisher and co-workers have argued that a generalization of revised scaling [14], known as "complete scaling" [25, 26], is appropriate for the description of liquid-vapor criticality. Complete scaling postulates that the theoretical fields, h, t, and Φ, are analytic functions of all the physical fields, $\Delta\mu$, ΔT, and ΔP. The Ising fields can then be expanded in the physical fields to yield,

$$\begin{aligned} h &= \Delta\mu + a_2\Delta T + a_3\Delta P + a_4(\Delta T)^2 + a_5\Delta\mu\Delta T + a_6(\Delta\mu)^2 + \cdots , \\ t &= \Delta T + b_2\Delta\mu + b_3\Delta P + b_4(\Delta T)^2 + b_5\Delta\mu\Delta T + b_6(\Delta\mu)^2 + \cdots , \\ \Phi &= \Delta P + c_2\Delta\mu + c_3\Delta T + c_4(\Delta T)^2 + c_5\Delta\mu\Delta T + c_6(\Delta\mu)^2 + \cdots , \end{aligned} \tag{1.32}$$

where the "$\cdots$" indicate higher order non-linear terms in the expansions. In addition to the revised scaling contribution, which is still controlled by b_2, there is a new leading contribution to the excess density,

$$\overline{\Delta\rho} \sim a_3|\Delta T|^{2\beta}, \tag{1.33}$$

where $2\beta \simeq 0.65$. As shown by Anisimov and Wang, and coworkers [27, 28], the combination of the 2β and $1-\alpha$ terms indeed accounts for the excess density data in asymmetric liquid-vapor systems and in liquid-liquid mixtures, even for strong asymmetry. By applying the isomorphism principle of critical phenomena [10, 11, 44], which states that liquid-vapor criticality can be consistently mapped onto criticality in liquid mixtures, to complete scaling, Wang *et al.* [29] have also shown that complete scaling describes asymmetry in liquid mixtures.

The complete scaling transformations, Eq. 1.32, also predict a Yang-Yang anomaly [25], *i. e.*, a divergence in the second temperature derivative of the chemical

potential at coexistence,

$$\left(\frac{d^2\hat{\mu}}{d\hat{T}^2}\right)_{\rm cxc} \sim -a_3|\Delta T|^{-\alpha}, \tag{1.34}$$

where the subscript "cxc", indicates that the derivative should be taken along the coexistence curve. This "anomaly" derives its name from the Yang-Yang relation [45],

$$\hat{\rho}\frac{\hat{C}_\rho}{\hat{T}} = \left(\frac{d^2\hat{P}}{d\hat{T}^2}\right)_{\rm cxc} - \hat{\rho}\left(\frac{d^2\hat{\mu}}{d\hat{T}^2}\right)_{\rm cxc}. \tag{1.35}$$

Thus, complete scaling predicts that the divergence of the isochoric heat-capacity is shared by both $\left(d^2\hat{P}/d\hat{T}^2\right)_{\rm cxc}$ and $\left(d^2\hat{\mu}/d\hat{T}^2\right)_{\rm cxc}$. Not surprisingly, complete scaling also predicts a new leading asymmetric correction to the isothermal susceptibility in the two phase region, namely,

$$\chi_T \approx \Gamma_0^- |\Delta T|^{-\gamma}\left(1 \pm 3a_3 B_0 |\Delta T|^{\beta}\right). \tag{1.36}$$

This summarizes the major asymmetry effects predicted by complete scaling for bulk systems. Tolman's length, an additional asymmetry effect associated with interfaces, will be discussed in Chap. 3.

1.3 Mean-field equations of state

To illustrate the concepts presented in the previous section, we will apply them to a particular EOS, the Landau expansion [46]. Mean-field equations of state, like the Landau expansion, do not properly treat fluctuations, and the critical behavior, while qualitatively correct, does not match the quantitative behavior of real systems. However, since the Landau expansion serves as the jumping off point for

more sophisticated theories and serves as an important limiting case, it is essential background material.

1.3.1 Ising model/Lattice Gas

A mean-field treatment of the Ising model near critical point, in which the spin at each lattice site feels only the average magnetization generated by the other spins, is equivalent to the Landau expansion of the Helmholtz energy. The Landau expansion is made by expanding $\Psi(m,t)$ in a Taylor series around the critical point, *i.e* for $t \ll 1$ and $m \ll 1$. To ensure that $\Psi(m) = \Psi(-m)$, only even powers of m appear in the expansion . We will also be interested in the mean-field role of fluctuations, and can approximate the energetic effects of spatial inhomogeneities by expanding in the magnetization gradient as well. Ψ is generally invariant under the spatial inversion $x \to -x$, so the square of the gradient is the first inhomogeneous contribution. The leading terms found by combining these elements are given by

$$\Psi \approx \Psi_0(t) + \frac{1}{2}|\nabla m|^2 + \frac{1}{2}tm^2 + \frac{g}{4!}m^4, \tag{1.37}$$

where $\Psi_0(t)$ is a function of temperature only. The constants in front of the $|\nabla m|^2$ and m^2 terms have been absorbed into definitions of the length scale and temperature scale respectively. The form of $\Psi_0(t)$ affects the entropy and the heat capacity, but not the magnetization or magnetic field. Many authors take $\Psi_0(t) = 0$. For this choice, the calculated heat capacity contains the background contribution $B_{\rm cr}$ introduced in Sec. 1.2.1. In order to focus on singular behavior in the critical region, we will take $\Psi_0(t) = -t^2/2g$, which eliminates $B_{\rm cr}$ in calculations. This is the standard

choice for field-theoretic calculations of critical phenomena [37].

The bulk thermodynamic equilibrium corresponds to $\nabla m = 0$. The magnetic field is given by

$$h = \left(\frac{\partial \Psi}{\partial m}\right)_t = tm + \frac{g}{6}m^3. \tag{1.38}$$

The magnetization at coexistence is found by solving the equation $h = 0$, with the result

$$m^{\pm} = \pm m_0 = \pm \left(\frac{6|t|}{g}\right)^{1/2}. \tag{1.39}$$

The entropy is

$$\Delta s = -\left(\frac{\partial \Psi}{\partial t}\right)_m = \frac{t}{g} - \frac{1}{2}m^2. \tag{1.40}$$

At coexistence, this becomes $\Delta s = -(4/g)|t|$. From this we see that the heat-capacity exhibits a jump discontinuity across the critical point, but does not diverge. The magnetic susceptibility, analogous to the isothermal susceptibility χ_T is defined by $\chi = (\partial m/\partial h)_t$, which yields

$$\chi^{-1} = t + \frac{g}{2}m^2. \tag{1.41}$$

In order to calculate the m-m correlation function from Eq. 1.37, we take $\nabla m \neq 0$. The fluctuation-disappation theorem [46] relates this correlation function to the Helmholtz energy Ψ by

$$\langle m(x)m(0)\rangle = \left(\frac{\delta^2 \Psi}{\delta m^2}\right)^{-1}, \tag{1.42}$$

where δ denotes a functional derivative. The Fourier transform of the correlation function defines a wavenumber dependent susceptibility

$$\chi(q) = \int dx e^{iqx} \langle m(x)m(0)\rangle = \frac{\chi}{1 + \xi^2 q^2}, \tag{1.43}$$

Exponent:	β	α	γ	ν	η	δ
Value:	1/2	0	1	1/2	0	3

Table 1.2: Mean-field critical exponents

Amplitude:	B_0	A_0^+	A_0^-	Γ_0^+	Γ_0^-	ξ_0^+	ξ_0^-
Value:	$\sqrt{6/g}$	$1/g$	$4/g$	1	1/2	1	$1/\sqrt{2}$

Table 1.3: Mean-field critical amplitudes

where, in the mean-field approximation, $\xi^2 = \chi$. The values of the critical exponents and amplitudes associated with the results of this section are listed in tables 1.2 and 1.3 respectively.

1.3.2 Asymmetric Landau expansion

For a liquid-vapor system, odd powers of the density are included in the Landau expansion. The asymmetric Landau expansion is given by

$$\hat{f} \approx f_0(T) + \frac{1}{2}|\nabla\hat{\rho}|^2 + \frac{1}{2}\Delta T\,(\Delta\rho)^2 + \frac{g}{4!}\,(\Delta\rho)^4 \tag{1.44}$$

$$+\mu_1(T)\Delta\rho + \frac{u_3}{3!}\Delta T\,(\Delta\rho)^3 + \frac{gu_5}{5!}\,(\Delta\rho)^5 \tag{1.45}$$

where $f_0(T) \approx \hat{f}_c - \hat{s}_c\Delta T - (\Delta T)^2/2g$ and $\mu_1(T) \approx \hat{\mu}_c + (u_1/g)\,(\Delta T)^2$. The leading behavior of the density is $\Delta\rho \sim |\Delta T|^{1/2}$, so that the new asymmetric terms are $O\left(|\Delta T|^{5/2}\right)$, where as the Ising terms are $O\left(|\Delta T|^2\right)$. Here, and throughout, the notation "$O(x)$" means "order x". At this order, an asymmetric gradient term

$-(u_\lambda/3!)(\Delta\rho)^2\nabla^2\hat{\rho}$ should also be included, but we reserve discussion of its effects for Chap. 3. Since the asymmetric terms produce corrections to the leading symmetric behavior, all results can be consistently linearized in u_1, u_3, and u_5.

The van der Waals equation is a famous mean-field EOS that describes the liquid-vapor transition. When this EOS is expanded around the critical point, explicit values for the coefficients of the asymmetric Landau expansion can be found. Due to a special symmetry $u_3 = 0$. The remaining coefficients are $g = 3/2$ and $gu_5 = -3/2$. The relative minus sign between these terms is a general feature of the asymmetric Helmholtz energy, and is not unique to the van der Waals EOS. The chemical potential coefficient u_1 cannot be determined from the EOS, but will not enter into any of the quantities we calculate.

Below the critical temperature, the equilibrium density along the critical isochore does not correspond to $\Delta\mu = 0$, as in the Ising case. Instead diffusive equilibrium requires $\mu(\rho = \rho^{\pm}) = \mu_{\rm cxc}(T)$ and material equilibrium requires $f(\rho^+, T) - \mu_{\rm cxc}(T)\rho^+ = f(\rho^-, T) - \mu_{\rm cxc}(T)\rho^-$. Solving these two equations simultaneously to first order in the asymmetry yields

$$\Delta\rho^{\pm} = \pm\Delta\rho_0 + (\Delta\rho_0)^2\left[\frac{u_3}{6} - \frac{u_5}{10}\right], \quad \Delta T < 0, \tag{1.46}$$

where $\Delta\rho_0 = (6|\Delta T|/g)^{1/2}$ is the symmetric result, and

$$\mu_{\rm cxc} = \left[\frac{3}{10}u_5 - u_3 + u_1\right]\frac{|\Delta T|^2}{g}, \quad \Delta T < 0. \tag{1.47}$$

The excess density therefore follows the law of rectilinear diameter. The asymmetric mean-field coexistence curve is plotted in Fig. 1.6. Above the critical point, $\Delta\rho = 0$

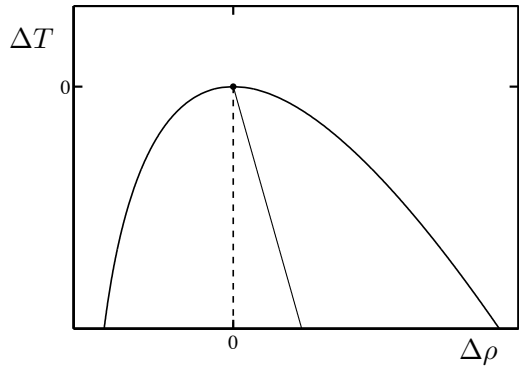

Figure 1.6: Schematic asymmetric mean-field coexistence curve

and $\mu(T) = (u_1/g)|\Delta T|^2$. Rather than diverging at the critical point, the second derivative of $\mu_{\rm cxc}$, like C_ρ, exhibits a jump discontinuity given by

$$\left(\frac{d^2\mu^-}{dT^2}\right) - \left(\frac{d^2\mu^+}{dT^2}\right) = -\frac{1}{g}\left[2u_3 - \frac{3}{5}u_5\right], \tag{1.48}$$

where the + and − denote the values above and below the critical point. The isothermal susceptibility matches the symmetric result above the critical point, but below one finds

$$\chi_T = \frac{1}{2|\Delta T|}\left(1 \mp \frac{1}{5}u_5\Delta\rho_0\right), \quad \Delta T < 0. \tag{1.49}$$

The chemical potential along the critical isotherm ($T = T_{\rm c}$) contains a similar asymmetric correction, so that

$$\mu = \frac{g}{6}\Delta\rho|\Delta\rho|^2\left(1 + \frac{1}{4}u_5\Delta\rho\right). \tag{1.50}$$

1.3.3 Complete scaling in mean-field approximation

Anisimov and Wang have shown the validity of complete scaling for the mean-field EOS, by demonstrating a mapping of the mean-field Ising EOS, Eq. 1.37, onto the asymmetric EOS, Eq. 1.45 via the complete scaling transformations [27, 28].

To this end, they worked with a simplified set of transformations, given by

$$\begin{aligned} h &= \Delta\mu + a\left[\Delta P - \hat{s}_{\rm c}\Delta T\right] \\ t &= \Delta T + b\Delta\mu \\ \Phi &= \Delta P - \hat{s}_{\rm c}\Delta T - \Delta\mu, \end{aligned} \tag{1.51}$$

where the asymmetry is fully characterized by the constants a and b. The relationship between the magnetization and the fluid density is found to be

$$\hat{\rho} = \frac{1 + m + b\Delta s}{1 - am}. \tag{1.52}$$

Wang and Anisimov chose $\Psi_0 = 0$ in Eq. 1.37, so that $\Delta s = -(1/2)m^2$. When $\Delta\rho$ is expanded to linear order in a and b, it simplifies to

$$\Delta\rho \simeq (1 + a)\, m + \left(a - \frac{1}{2}b\right) m^2. \tag{1.53}$$

In the mean-field approximation, 2β and $1 - \alpha$ are both 1. The temperature can also be written in terms of the symmetric variables as

$$\Delta T = t - b\left(tm + \frac{g}{6}m^3\right). \tag{1.54}$$

When these expressions for the density and temperature are substituted in Eq. (1.45) for Δf, with $u_1 = 0$, the symmetric Ψ, Eq. (1.37), is reproduced if

$$a = \frac{2}{3}u_3 - \frac{1}{5}u_5, \quad b = u_3 - \frac{1}{5}u_5, \tag{1.55}$$

and if the temperature scale and the coupling constant are rescaled as

$$\Delta T \to (1 - 2a)\Delta T, \quad g \to (1 - 4a)g. \tag{1.56}$$

At the level of mean-field theory, this shows that complete scaling accurately maps the symmetric Ising model onto an asymmetric liquid-vapor system.

Chapter 2

Complete scaling and the renormalization group

2.1 Introduction

As discussed in Sec. 1.2.3, at least two different theoretical approaches have been used to investigate asymmetric fluid criticality. The RG approach to asymmetric fluid criticality combines the results of revised scaling with a new asymmetric correction to scaling exponent, which leads the excess density

$$\overline{\Delta\rho} \sim D_{1-\alpha}|\Delta T|^{1-\alpha} + D_1|\Delta T| + D_{\theta_5}|\Delta T|^{\beta+\theta_5} + \cdots , \tag{2.1}$$

where $\overline{\Delta\rho}$ was defined in Eq. 1.28. RG techniques have the advantage of a solid theoretical underpinning. For the symmetric case, RG based predictions of critical phenomena, including the symmetric corrections to scaling, have been exremely successful. It is hard to believe that asymmetric corrections are so fundamentally different that they break from this mold. Furthermore, the validity of revised scaling, which produces the $1-\alpha$ term, has been demonstrated by Nicoll [24]. The shortcomings of his treatment appear to be the uncertainty in the value of θ_5, and the failure to fully explain experiments as discussed by Anisimov and Wang [28, 29].

The complete scaling approach builds on the field-mixing of revised scaling, by adding pressure mixing. Complete scaling predicts that the excess density varies

as

$$\overline{\Delta\rho} \sim D_{2\beta}|\Delta T|^{2\beta} + D_{1-\alpha}|\Delta T|^{1-\alpha} + D_1|\Delta T| + \cdots . \tag{2.2}$$

The new leading 2β term agrees with the available liquid-vapor and liquid-liquid coexistence data [28, 29], but the mechanism of pressure mixing does not have a rigorous theoretical basis, except for the mean-field EOS, *cf.* Sec. 1.3.3, and for some exactly soluble models [47, 48]. However, the RG treatment also reproduces the mean-field EOS in the appropriate limit, so this can hardly be viewed as an acid test. In addition to the prediction of the 2β term in diameter, complete scaling predicts a Yang-Yang anomaly, whereas the RG approach developed by Nicoll, does not. These contradictions have not been adequately addressed in the literature. Authors either treat the RG as inadequate to the problem and ignore the θ_5 contribution [28], or take complete scaling to represent physics beyond the RG treatment of the asymmetric LGW Hamiltonian and include θ_5 as an additional higher order correction [26]. If both theories reproduce the same mean-field EOS, one would intuitively expect that they might not be so dissimilar. Clearly, either the RG treatment or complete scaling produce an incomplete description of fluid criticality. It is therefore desirable to reconcile, or at least understand, the differences between them.

One of the reasons that a direct comparison between the two theories has not been previously made is that they are presented in different languages. Complete scaling primarily deals with macroscopic thermodynamic properties without necessarily making reference to a particular equation of state. Whereas the RG approach

seeks to calculate macroscopic properties from approximate mesoscopic interactions, *i.e.* the LGW Hamiltonian. A first step in making a comparison of the two is to imbed both in similar language.

In this chapter we investigate the connection between complete scaling and the RG approach to fluid asymmetry. In Sec. 2.2, complete scaling is expressed in a compact form and the EOS implied by complete scaling is derived. This EOS is then calculated to $O(\epsilon)$. Next, in Sec. 2.3, a derivation of an asymmetric EOS based on an RG analysis of an asymmetric LGW Hamiltonian is presented in the one-loop approximation. For brevity we will refer to this as the "asymmetric RG EOS" when comparing it to the complete scaling EOS. The derivation of the asymmetric RG EOS closely follows the derivation of the Ising-type EOS presented in Appendix A. The calculated complete scaling EOS and asymmetric RG EOS are then compared in Sec. 2.4, and are shown to be identical. This demonstrates the consistency of complete scaling at $O(\epsilon)$. The complete scaling prediction for the excess density is then fit to liquid-vapor data in Sec. 2.5, and the results are interpreted in light of the connection to the asymmetric RG EOS. The results of this chapter are summarized in Sec 2.6.

2.2 Complete scaling equation of state

In Eq. 1.32, complete scaling is presented as a set of transformations between physical and theoretical thermodynamic fields, in which all fields stand on equal footing. In this way, a distinction is made between linear and non-linear contribu-

tions to the complete scaling equations. Treating all fields as equal in this sense can be misleading. The temperature dependences of fields unambiguously distinguish them, since we have $\Delta T \sim O(\Delta T)$, $\Delta\mu \sim O(\Delta T^{2-\alpha-\beta})$, and $\Delta P \sim O(\Delta T^{2-\alpha})$. The reduced temperature is an important expansion parameter in critical phenomena, and thus, powers of the reduced temperature, in addition to the fields themselves, can be taken into consideration when formulating complete scaling. This viewpoint suggests two non-linear modifications of the simplified transformations, Eq. 1.51. First, a non-linear ΔT^2 should be included where ΔP is included. This term can be taken as part of $\hat{P}_{\rm r}$, the regular part of the pressure. If symmetric fields, h, t, and Φ, are expanded in the critical portion of the pressure $\Delta\tilde{P}$, as defined by Eq. 1.24, instead of ΔP as was done in Eq. 1.32, then the simplified transformations, Eq. 1.51, may be rewritten as

$$\begin{aligned} h &= \Delta\mu + a\Delta\tilde{P} \\ t &= \Delta T + b\Delta\mu \\ \Phi &= \Delta\tilde{P}, \end{aligned} \tag{2.3}$$

where a and b are constant mixing-parameters. As we will see shortly, expanding in $\Delta\tilde{P}$, instead of ΔP, removes the awkward pre-factor of $(1+a)$ from Eq. 1.53.

The leading asymmetric corrections to $\overline{\Delta\rho}$, χ_T, and $\mu_{\rm cxc}$ are smaller than the leading symmetric terms by a factor of $O(\Delta T^{\beta})$. This type of hierarchy may also be mirrored in the field-mixing. For this reason, we will consider an additional contribution $\Delta T\Delta\mu \sim O(\Delta T^{3-\alpha-\beta})$ to Φ, so that the full complete scaling transformations

can now be written

$$\begin{aligned} h &= \Delta\mu + a\Delta\tilde{P} \\ t &= \Delta T + b\Delta\mu \\ \Phi &= \Delta\tilde{P} + c\Delta T\Delta\mu, \end{aligned} \tag{2.4}$$

where c is a "new" mixing parameter. The cross-term $\Delta T\Delta\mu$ was included in the full transformations (Eq. 1.32) found by expanding Φ, but its role as a leading correction was not highlighted. In particular it was omitted from the simplified complete scaling transformations of Anisimov and Wang given by Eq. 1.51. The density is now,

$$\Delta\rho \simeq m + am^2 + b\Delta s - ct. \tag{2.5}$$

As previously mentioned, the switch from ΔP to $\Delta\tilde{\rho}$ removes the $(1+a)$ prefactor found in Eq. 1.53, and therefore eliminates the need to rescale ΔT and g, *cf.* Eq. 1.56. The new term, which is proportional to $|\Delta T|$, does not produce any qualitatively different effects. However, it is essential for the consistency of the theory and for adequate fitting to experimental data. Terms added at the next order of the hierarchy generate symmetric corrections to $\Delta\rho$. These include, $\Delta T\Delta\mu$ in h, and $\Delta T\Delta\tilde{P}$ and $\Delta\tilde{P}$ in t.

Complete scaling provides a total thermodynamic description, and therefore generates an equation of state. The EOS implied by the complete scaling transformations can be derived from a known expression for $\Phi(h,t)$. The exact expression for the complete scaling EOS will differ depending on the representation of $\Phi(h,t)$. There are a few natural representations, developed for the critical region of fluids,

such as the parametric models [8] and the more explicit ϵ-expansion. Expressing complete scaling as an EOS has two distinct advantages. All thermodynamic properties can be calculated systematically from an EOS, and an EOS can be compared with other equations of state, namely the asymmetric RG EOS found by Nicoll.

The transformations, Eq. 2.4, are expressed in terms of the pressure, chemical potential, and temperature. For this choice of variables, it is natural to develop an EOS for $\Delta P(\Delta\mu, \Delta T)$ rather than $\Delta\mu(\Delta P, \Delta T)$ or $\Delta T(\Delta\mu, \Delta P)$. The third relation in Eq. 2.4, rearranged as,

$$\Delta\tilde{P} = \Phi - c\Delta T\Delta\mu, \tag{2.6}$$

is essentially already in the desired form, except for the symmetric potential Φ, which is assumed to be a known function of h and t. The goal then is to re-express Φ as a function of $\Delta\mu$ and ΔT. To this end, the potential Φ can be expanded to linear order in asymmetric terms as

$$\Phi\left(h,t\right) \simeq \Phi|_0 + \left.\frac{\partial\Phi}{\partial h}\right|_0 \left(h-\Delta\mu\right) + \left.\frac{\partial\Phi}{\partial t}\right|_0 \left(t-\Delta T\right), \tag{2.7}$$

where the expansion is made around the point $h = \Delta\mu$ and $t = \Delta T$, *i.e.*

$$\Phi|_0 = \Phi\left(h=\Delta\mu, t=\Delta T\right). \tag{2.8}$$

By definition, $m|_0 = \partial\Phi/\partial h|_0$ and $\Delta s|_0 = \partial\Phi/\partial t|_0$, so that Eq. (2.6) can now be written as

$$\Delta\tilde{P} = \left(1+am|_0\right)\Phi|_0 + \left(b\Delta s|_0 - c\Delta T\right)\Delta\mu. \tag{2.9}$$

In the above expression $m|_0$, $\Delta s|_0$, and $\Phi|_0$ are to be considered functions of $\Delta\mu$ and ΔT. The pressure, ΔP, has now been fully expressed as a function of $\Delta\mu$ and

ΔT. For instance, if the potential Φ is presented in the form of the scaling EOS, Eq. 1.17, namely,

$$\Phi|_0 = |\Delta T|^{2-\alpha} X^{\pm}(x), \tag{2.10}$$

where $x = \Delta\mu/|\Delta T|^{\beta+\gamma}$, the densities are then

$$m|_0 = |\Delta T|^{\beta} X'(x) \tag{2.11}$$

$$\Delta s|_0 = |\Delta T|^{1-\alpha}\left[(2-\alpha)X^{\pm}(x) - (\beta+\gamma)\frac{\Delta\mu}{|\Delta T|^{\beta+\gamma}}X'(x)\right], \tag{2.12}$$

where X' is the derivate of $X^{\pm}$ with respect to its argument. Putting these pieces together yields

$$\begin{aligned}\Delta\tilde{P} &= |\Delta T|^{2-\alpha}X^{\pm} + a|\Delta T|^{2-\alpha+\beta}\left[X^{\pm} + xX'\right]X' \\ &+ b|\Delta T|^{1-\alpha+\beta+\gamma}\left[(2-\alpha)xX^{\pm} - (\beta+\gamma)x^2X'\right] \\ &+ c|\Delta T|^{1+\beta+\gamma}x.\end{aligned} \tag{2.13}$$

This expression is cumbersome and does not easily yield explicit results for the quantities of interest. The same is not true of the Helmholtz energy. RG calculations are conveniently expressed in terms of the density $\Delta\rho$ and temperature ΔT and lend themselves to the calculation of Helmholtz energy. It is more illuminating to work with the complete scaling EOS for the Helmholtz energy, $f(\Delta\rho, \Delta T)$.

2.2.1 Equation of state for the Helmholtz energy

The derivation of the complete scaling Helmholtz energy closely follows the derivation of the pressure with a few modifications. When inverted, the complete

scaling transformations become

$$\begin{aligned} \Delta\mu &= h - a\Phi, \\ \Delta T &= t - bh, \\ \Delta\tilde{P} &= \Phi - cth. \end{aligned} \tag{2.14}$$

The definition of the free energy, $f = \mu\rho - P$, and these inverse transformations can be combined with Eq. 2.5 to yield

$$\begin{aligned} \Delta T &= t - bh, \\ \Delta\rho &= m + am^2 + b\Delta s - ct, \\ \Delta\tilde{f} &= (1 + am)\,\Psi + b(\Delta s)h, \end{aligned} \tag{2.15}$$

where the critical portion of the Helmholtz energy $\Delta\tilde{f}$ is defined in Eq. 1.25. These are the complete scaling relations for the Helmholtz energy and its natural variables. We want an EOS for $f(\Delta\rho, \Delta T)$ and therefore expand the quantities on the right hand side of the third equation around the symmetric solution defined by $m = \Delta\rho$ and $t = \Delta T$. The expansion of Ψ is

$$\Psi\,(m,t) \simeq \Psi|_0 + \left.\frac{\partial\Psi}{\partial m}\right|_0 (m - \Delta\rho) + \left.\frac{\partial\Psi}{\partial t}\right|_0 (t - \Delta T)\,. \tag{2.16}$$

The complete scaling Helmholtz energy is therefore given by

$$\Delta\tilde{f} = (1 + a\Delta\rho)\,\Psi|_0 - \left(a\Delta\rho^2 + b\Delta s|_0 - c\Delta T\right) h|_0 \tag{2.17}$$

where $h|_0$, $\Delta s|_0$, and $\Psi|_0$ are assumed to be known functions of $\Delta\rho$ and ΔT. Given an EOS for the symmetric system, $\Psi|_0$, the expressions for $s|_0$ and $h|_0$ can be calculated and then substituted into Eq. 2.17 to generate an explicit complete scaling EOS in terms of the three asymmetry parameters, a, b, and c.

2.2.2 Linear model

A popular equation of state used for the description of critical phenomena is the linear parametric model [49]. This model has been shown to match the Ising-type EOS to $O(\epsilon^2)$ [50]. The linear model expresses the distance to the critical point in terms of the variables r and θ, which are defined by the relations

$$\Delta\rho = k\theta r^{\beta} \tag{2.18}$$

$$\Delta T = r\left(1 - b_{\text{L}}^2\theta^2\right) \tag{2.19}$$

where b_{L} and k are constants. The linear model EOS is given by

$$\Psi = a_{\text{L}} k r^{2-\alpha}\psi(\theta) + \frac{1}{2}B_{\text{cr}}r^2\left(1 - b_{\text{L}}^2\theta^2\right) \tag{2.20}$$

where $\psi(\theta)$ is known function of θ, a_{L} is constant, and B_{cr} is the critical heat capacity background [51]. The expression for the field and entropy are easily derived from this,

$$h = a_{\text{L}} r^{2-\alpha-\beta}\theta\left(1 - \theta^2\right) \tag{2.21}$$

$$\Delta s = a_{\text{L}} k r^{1-\alpha} s(\theta) - a_{\text{L}} k r\left(1 - b_{\text{L}}^2\theta^2\right)/3, \tag{2.22}$$

where $s(\theta)$ is related to $f(\theta)$ and the critical exponents. The complete scaling EOS based on the linear model can then be found by substituting these expressions into Eq. 2.17.

2.2.3 ϵ-expansion

The complete scaling EOS can be developed in an explicit ϵ-expansion by using the Ising-type EOS derived in the one loop-approximation. A brief derivation

of this EOS is presented in Appendix A. The universal asymptotic critical behavior of the Ising model can be found from an EOS resulting from the RG analysis of a symmetric one-component LGW Hamiltonian. For the remainder of this work, "Ising-type" or "Ising" should be understood to refer to this particular EOS, and not the actual 3D Ising-model. The Ising-type Helmholtz energy, magnetic field, and entropy are

$$\Psi|_0 = -\frac{1}{2}\frac{(\Delta T)^2}{g} + \frac{1}{2}\Delta T\,(\Delta\rho)^2 + \frac{g}{4!}\,(\Delta\rho)^4 + \frac{\epsilon}{24}\left(\frac{\kappa^4}{g}\right)(2L+1)\,, \quad (2.23)$$

$$h|_0 = \Delta T\Delta\rho + \frac{g}{6}\,(\Delta\rho)^3 + \frac{\epsilon}{6}(\Delta\rho)\kappa^2\,(L+1)\,, \quad (2.24)$$

$$\Delta s|_0 = \frac{\Delta T}{g} - \frac{1}{2}\,(\Delta\rho)^2 - \frac{\epsilon}{6}\left(\frac{\kappa^2}{g}\right)(L+1)\,, \quad (2.25)$$

where

$$\kappa^2 = \Delta T + \frac{g}{2}\,(\Delta\rho)^2 \quad (2.26)$$

and

$$L = \ln\kappa^2. \quad (2.27)$$

The mean-field expressions can be recovered by neglecting the fluctuation corrections, i.e, taking $\epsilon \to 0$. The expressions for the fluctuation corrections can be divided into universal and non-universal contributions. At this order, the universal portions determine the critical exponents and are proportional to L, whereas the non-universal portions are not proportional to L, and contribute to the critical amplitudes. The entropy in Eq. 2.25 corresponds to

$$\Delta s|_0 \approx \frac{A_0^-}{1-\alpha}\Delta T|\Delta T|^{-\alpha}, \quad (2.28)$$

without the critical background $B_{\rm cr}|\Delta T|$. Previous work on complete scaling has included the background term in the entropy, *cf.* Sec. 1.3.3. The corresponding results will be compared with those based on Eqs. 2.23-2.25 at the end of the chapter.

The asymmetric Helmholtz energy resulting from the combination of Eq. 2.17 and the Eqs. 2.23-2.25 can be cast into the form of a Landau expansion in $\Delta\rho$ as

$$\begin{aligned}\Delta\tilde{f} &= f_0\frac{(\Delta T)^2}{g} + \frac{1}{2}f_2\Delta T\,(\Delta\rho)^2 + \frac{1}{4!}f_4\,(\Delta\rho)^4 \\ &+ f_1\frac{(\Delta T)^2}{g}\Delta\rho + \frac{1}{3!}f_3\Delta T\,(\Delta\rho)^3 + \frac{1}{5!}f_5\,(\Delta\rho)^5 \end{aligned} \tag{2.29}$$

The coefficients for even powers of $\Delta\rho$ match those of the Ising-type EOS presented in Appendix A, and are

$$\begin{aligned} f_0 &= -\frac{1}{2}\left[1-\frac{\epsilon}{6}(L+1)\right], \\ f_2 &= 1+\frac{\epsilon}{6}(L+1), \\ f_4 &= g\left[1+\frac{\epsilon}{2}(L+1)\right]. \end{aligned} \tag{2.30}$$

If

$$\hat{a} = a(1+\epsilon/12), \tag{2.31}$$

and

$$\hat{c} = gc, \tag{2.32}$$

the asymmetric coefficients can be written,

$$\begin{aligned} f_1 &= (\hat{c}-b-\frac{1}{2}\hat{a}) + \frac{\epsilon}{12}\,(a+2\hat{c})\,(L+1), \\ f_3 &= (2b-3\hat{a}+\hat{c}) + \frac{\epsilon}{6}\left(\frac{2}{3}b-3a+3\hat{c}\right)(L+1), \\ f_5 &= g\left[(10b-15\hat{a}) + \frac{\epsilon}{6}\,(40b-45a)\,(L+1)\right]. \end{aligned} \tag{2.33}$$

We will now illustrate the way in which Eq. 2.29 reproduces the expected complete scaling results. To simplify the presentation, we will only consider the universal portions of the EOS. The non-universal complete scaling results are also correctly reproduced, however, their presence leads to undue clutter. Along the critical isochore, $\kappa^2 \sim |\Delta T|$. Therefore, the universal portions of the coefficients in Eq. 2.29 can be isolated by taking $(L+1) \to \ln|\Delta T|$. The complete scaling EOS then looks like the asymmetric mean-field EOS, Eq. 1.45, but with temperature dependent coefficients. The chief asymmetric properties of interest, namely, $\overline{\Delta\rho}$, $\mu_{\rm cxc}$, χ_T, are calculated by taking density derivatives of the Helmholtz energy along the critical isochore. Thus, the universal parts of these properties can be found using the mean-field expressions. The results will reproduce the critical exponents to $O(\epsilon)$, and the mean-field amplitudes. The mean-field formula for the excess density is

$$\overline{\Delta\rho} = \left(\frac{6f_2|\Delta T|}{f_4}\right)\left[\frac{1}{6}\frac{f_3}{f_2} - \frac{1}{10}\frac{f_5}{f_4}\right]. \tag{2.34}$$

The expansion coefficient ratios appearing in this formula are given to linear order in ϵ by,

$$\frac{f_2}{f_4} = \frac{1+\frac{\epsilon}{6}\ln|\Delta T|}{g(1+\frac{\epsilon}{2}\ln|\Delta T|)} \simeq \frac{1}{g}(1-\frac{\epsilon}{3}\ln|\Delta T|) \tag{2.35}$$

$$\begin{aligned}\frac{f_3}{f_2} &= \frac{2b-3a-c}{1+\frac{\epsilon}{6}\ln|\Delta T|} + \frac{\epsilon}{6}(4b-3a-3c)\ln|\Delta T| \\ &\simeq (2b-3a-c) + \frac{\epsilon}{6}(2b-2c)\ln|\Delta T|\end{aligned} \tag{2.36}$$

$$\begin{aligned}\frac{f_5}{f_4} &= \frac{10b-15a}{1+\frac{\epsilon}{2}\ln|\Delta T|} + \frac{\epsilon}{6}(40b-45a)\ln|\Delta T| \\ &\simeq (10b-15a) + \frac{\epsilon}{6}(10b)\ln|\Delta T|.\end{aligned} \tag{2.37}$$

When these ratios are substituted into Eq. 2.34, we find

$$\overline{\Delta\rho} = \frac{6|\Delta T|}{g}\left(1 - \frac{\epsilon}{3}\ln|\Delta T|\right)\left[a - \frac{2}{3}b\left(1 + \frac{\epsilon}{6}\ln|\Delta T|\right)\right] + c|\Delta T| \tag{2.38}$$

The ϵ-expansion is interpreted through the relation

$$|\Delta T|^{\epsilon} \simeq 1 + \epsilon \ln|\Delta T|. \tag{2.39}$$

This interpretation of Eq. 2.38 leads naturally to the expected complete scaling result,

$$\overline{\Delta\rho} = a\,(B_0)^2\,|\Delta T|^{2\beta} - b\frac{A_0^-}{1-\alpha}|\Delta T|^{1-\alpha} + c|\Delta T|, \tag{2.40}$$

where we have made use of the mean-field critical amplitudes, and the values of the critical exponents at $O(\epsilon)$ listed in Appendix A.

The general mean-field expression for the chemical potential at coexistence is

$$\mu_{\rm cxc} = \left[\frac{3}{10}\frac{f_5}{f_4} - \frac{f_3}{f_2}\right]\frac{(f_2|\Delta T|)^2}{f_4} + f_1\frac{(|\Delta T|)^2}{g} \tag{2.41}$$

When the coefficients are substituted into this equation the result simplifies to

$$\mu_{\rm cxc} = -2a\frac{(|\Delta T|)^2}{g}\left(1 - \frac{\epsilon}{6}\ln|\Delta T|\right), \tag{2.42}$$

which can be rewritten to $O(\epsilon)$ as

$$\mu_{\rm cxc} = -\frac{a}{(2-\alpha)}\left(\frac{A_0^-}{1-\alpha}\right)|\Delta T|^{2-\alpha}. \tag{2.43}$$

The mean-field isothermal susceptibility is

$$\chi_T = \frac{1}{2f_2|\Delta T|}\left(1 \mp \frac{1}{5}\frac{f_5}{f_4}\left(\frac{6f_2|\Delta T|}{f_4}\right)^{1/2}\right)., \tag{2.44}$$

which interpreteted as

$$\chi_T = \Gamma_0^-|\Delta T|^{-\gamma}\left(1 \pm \left[3a|\Delta T|^{\beta} - 2b\frac{\beta}{\Gamma_0^-}|\Delta T|^{1-\alpha-\beta}\right]B_0\right), \tag{2.45}$$

where the mean-field relation $\beta/\Gamma_0^- = 1$ has been used to match the previous complete scaling resutls.

The Landau-type expansion of the complete scaling EOS, Eq. 2.29, can also be used to find the behavior of the chemical potential along the critical isotherm. Along the critical isotherm, $\kappa^2 = \frac{g}{2}(\Delta\rho)^2$, therefore we can write, $L = \ln|\frac{g}{2}| + \ln|(\Delta\rho)^2|$. The first term can be neglected in the present analysis because it only makes a non-universal contribution. Now, to isolate the universal component, we take $(L+1) \rightarrow \ln|(\Delta\rho)^2|$. The mean-field expression is given by

$$\mu = \left(\frac{f_4}{6}\right)\Delta\rho|\Delta\rho|^2\left(1 \pm \frac{1}{4}\frac{f_5}{f_4}\Delta\rho\right). \tag{2.46}$$

When the coefficients are substituted into this expression we obtain

$$\mu \sim \Delta\rho|\Delta\rho|^{\delta-1}\left(1 - \frac{15}{4}a\Delta\rho - \frac{5}{2}b\Delta\rho|\Delta\rho|^{(\gamma-1)/\beta}\right). \tag{2.47}$$

This result is not typically calculated in presentations of complete scaling. All of these results demonstrate the consistency of the complete scaling EOS at least in the one-loop approximation.

2.3 RG treatment of fluid asymmetry

In this section an asymmetric EOS is calculated from a RG analysis of an asymmetric LGW Hamiltonian in the one-loop approximation. Several other authors have also treated this issue. Wegner [20] and Ley-Koo and Green [22] made their analyses based on the Wegner expansion. Vause and Sak [21] derived an asymmetric EOS, but for a limited form of the Hamiltonian. The most comprehensive treatment

has been provided by Nicoll and Zia [23] and Nicoll [24], who made an RG treatment and considered the most general form of the Hamiltonian. Our calculation differs slightly in approach from Nicoll's, but arrives at the same EOS.

The terms appearing in the Ising-type LGW Hamiltonian, presented in Appendix A, are restricted by the symmetry requirement $\mathcal{H}_I[\phi] = \mathcal{H}_I[-\phi]$, where ϕ is the field-variable. This ensures that only even powers of ϕ appear in the Hamiltonian. Fluids are not bound by this requirement, and additional operators need to be added to construct a general asymmetric Hamiltonian. The full asymmetric LGW Hamiltonian has the form $\mathcal{H} = \mathcal{H}_I + \mathcal{H}_A$, where $\mathcal{H}_I$ is the Ising-type LGW Hamiltonian, and

$$\mathcal{H}_A = u_1^0 O_1 + u_3^0 O_3 + u_5^0 O_5 + u_\lambda^0 O_\lambda, \tag{2.48}$$

where the operators, O_i, are given by

$$O_1 = \frac{(\Delta T_0)^2}{g_0}\phi, \quad O_3 = \frac{1}{3!}\Delta T_0 \phi^3, \tag{2.49}$$

$$O_5 = \frac{g_0}{5!}\phi^5, \quad O_\lambda = -\frac{1}{3!}\phi^2 \nabla^2 \phi. \tag{2.50}$$

The necessity of the asymmetric gradient operator, O_λ, was one of the key insights of Nicoll and Zia's work. In the Ising-type LGW Hamiltonian, the gradient can be written either as $(1/2)|\nabla\phi|^2$ or $-(1/2)\phi\nabla^2\phi$. There is a similar flexibility in how the asymmetric gradient is written. Integrating $-(1/3!)\phi^2\nabla^2\phi$ by parts, we find that it is equivalent to $(1/3)\phi|\nabla\phi|^2$ up to a total divergence, which will not affect any of the results.

The reduced density is related to ϕ by, $\Delta\rho = \langle\phi\rangle$, where the bracket denotes an average. Hence, we see that $\mathcal{H}[\langle\phi\rangle] = \Delta\bar{f}$, where $\Delta\bar{f}$ is the asymmetric mean-field

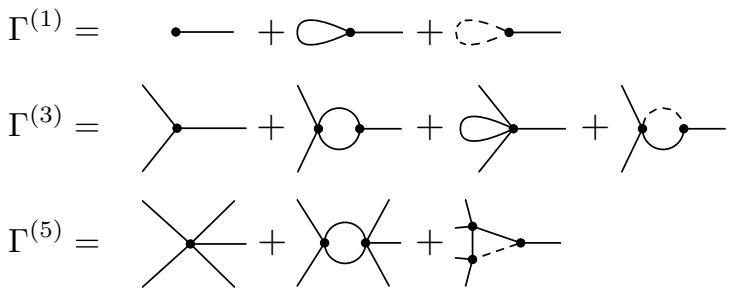

Figure 2.1: Asymmetric vertex-function diagrams up to one loop

EOS, Eq 1.37, if $u_i = u_i^0$. In the mean-field EOS, the terms in $\mathcal{H}_A$ are all of order $|\Delta T|^{5/2}$, and are therefore higher order than the Ising terms, which are of order $|\Delta T|^2$. In this sense, $\mathcal{H}_A$ is a perturbation to $\mathcal{H}_I$, and the leading asymmetry effects are captured by working to linear order in the coupling constants u_i.

Nicoll and Zia have previously shown that the addition of asymmetric terms to the Hamiltonian does not destabilize the Ising fixed-point [23]. Hence, the derivation of the asymmetric EOS follows the derivation of the Ising-type EOS from a LGW Hamiltonian. In addition to the Ising normalization conditions, there are three additional conditions that serve to renormalize the asymmetric coupling constants

$$\begin{aligned}
\Gamma^{(1)}\left(p_1;\{\nu_i^0\}\right)\big|_{p_1=0} &= u_1(\Delta T)^2/g, \\
\Gamma^{(3)}\left(p_1,p_2,p_3;\{\nu_i^0\}\right)\big|_{p_i=0} &= u_3\Delta T, \\
\Gamma^{(5)}\left(p_1,\ldots,p_5;\{\nu_i^0\}\right)\big|_{p_i=0} &= gu_5.
\end{aligned} \tag{2.51}$$

The diagramatic expansions of the vertex functions are given in Fig. 2.1. Reading

off the terms in Fig. 2.1, we find

$$\begin{aligned} u_1 &= u_1^0 - u_3^0\left(\frac{g_o}{2}J\right) + u_\lambda^0\left(\frac{g_o}{3}J\right), \\ u_3 &= u_3^0\left(1 - \frac{3}{2}g_0 J\right) - u_5^0\left(\frac{g_0}{2}J\right) + u_\lambda^0(2g_0 J), \\ u_5 &= u_5^0\left(1 - 5g_0 J\right) + u_\lambda^0(10g_0 J), \end{aligned} \tag{2.52}$$

where the so-called "mass shift", has been omitted, and where we take

$$J \approx \frac{1}{\epsilon}\left(1 + \frac{\epsilon}{2}\right). \tag{2.53}$$

The explanation and justification of this choice of J are identical to those given in Appendix A for the Ising-type EOS. The bare coefficients u_1^0, u_3^0, and u_5^0 are found by inverting Eq. 2.52 for the renormalized coefficients to linear order in g as

$$\begin{aligned} u_1^0 &= u_1 + u_3\left(\frac{g}{2}J\right) - u_\lambda\left(\frac{g}{3}J\right), \\ u_3^0 &= u_3\left(1 + \frac{3}{2}gJ\right) + u_5\left(\frac{g}{2}J\right) - u_\lambda(2gJ), \\ u_5^0 &= u_5\left(1 + 5gJ\right) - u_\lambda(10gJ). \end{aligned} \tag{2.54}$$

The EOS in the one-loop approximation is

$$\Delta\tilde{f} = \mathcal{H}|_{\phi=\Delta\rho} + \frac{1}{2}\mathrm{Tr}\left\{\ln\mathcal{H}^{(2)}\right\}. \tag{2.55}$$

The fluctuation operator, $\mathcal{H}^{(2)} = \delta^2\mathcal{H}/\delta\phi^2|_{\phi=\Delta\rho}$, takes the form

$$\mathcal{H}^{(2)} = \left[-\psi\nabla^2 + \bar{f}''\right]\delta(x_1 - x_2). \tag{2.56}$$

where

$$\psi = \left(1 + \frac{2}{3}u_\lambda\Delta\rho\right), \tag{2.57}$$

and

$$\bar{f}'' = \left(\frac{\partial^2 \bar{f}}{\partial \rho^2}\right)_T = \Delta T + \frac{g}{2}\Delta\rho^2 + u_3 \Delta T \Delta\rho + \frac{g u_5}{6}\Delta\rho^3 \tag{2.58}$$

where $\bar{f}$ is the mean-field Helmholtz energy, given in Eq. 1.45. Note that u_1 does not enter into the fluctuation operator. The fluctuation correction is given by

$$\frac{1}{2}\mathrm{Tr}\ln\mathcal{H}^{(2)} = \frac{1}{2}\int_p \ln\left[\psi p^2 + \bar{f}''\right] = -\frac{1}{4\epsilon}\left(1 - \frac{\epsilon}{4}\right)^{-1}\left(\frac{\bar{f}''}{\psi}\right)^{2-\epsilon/2}, \tag{2.59}$$

where the integration has been performed in $d = 4 - \epsilon$ dimensions. To linear order in the asymmetry,

$$\begin{aligned}\frac{1}{g}\left(\frac{\bar{f}''}{\psi}\right)^2 &\simeq \left(\Delta T + \frac{g}{2}\Delta\rho^2\right)^2 + \left(2u_3 - \frac{4}{3}u_\lambda\right)\frac{(\Delta T)^2}{g}\Delta\rho \\ &+ \left(u_3 + \frac{1}{3}u_5 - \frac{4}{3}u_\lambda\right)\Delta T\,(\Delta\rho)^3 + g\left(\frac{1}{6}u_5 - \frac{1}{3}u_\lambda\right)(\Delta\rho)^5. \end{aligned}\tag{2.60}$$

The Hamiltonian, expressed in terms of the renormalized coefficients, is therefore

$$\mathcal{H}|_{\phi=\Delta\rho} = \frac{1}{4}\left(\frac{\bar{f}''}{\psi}\right)^2 J. \tag{2.61}$$

By expanding to first order in ϵ, we can write the total Helmholtz energy as

$$\Delta\tilde{f} = \bar{f} + \frac{\epsilon}{24g}\left(\frac{\bar{f}''}{\psi}\right)^2\left\{2\ln\left(\frac{\bar{f}''}{\psi}\right) + 1\right\} \tag{2.62}$$

This is identical to the Ising-type EOS presented in Appendix A, but with the Ising $\bar{\Psi}''$ (of κ^2) replaced by $\bar{f}''/\psi$, *cf.* Eq. A.24. This result can be further simplified by expanding to linear order in the asymmetry to obtain

$$\begin{aligned}\Delta\tilde{f} = \bar{f} &+ \frac{\epsilon}{24}\left(\frac{\kappa^4}{g}\right)(2L+1) \\ &+ \frac{\epsilon}{6}\left(\frac{\kappa^2}{g}\right)\Delta\rho\left[u_3\Delta T + \frac{g u_5}{6}\Delta\rho^2 - \frac{2}{3}u_\lambda\kappa^2\right](L+1), \end{aligned}\tag{2.63}$$

where $\kappa^2 = \Delta T + \frac{g}{2}(\Delta\rho)^2$ and $L = \ln \kappa^2$ were previously defined in Eqs. 2.26 and 2.27. This matches Nicoll's result at $O(\epsilon)$ exactly. In the symmetric limit, $u_1 = u_3 = u_5 = u_\lambda = 0$, the Ising-type EOS (Eq. 2.23) is reproduced.

This result can also be cast into the form of a Landau expansion by gathering together like powers of $\Delta\rho$. The results from the Ising-type EOS, Eq. 2.30, are recovered for f_0, f_2, and f_4, and the asymmetric coefficients are found to be

$$\begin{aligned} f_1 &= u_1 + \frac{\epsilon}{6}\left(u_3 - \frac{2}{3}u_\lambda\right)(L+1), \\ f_3 &= u_3 + \frac{\epsilon}{2}\left(u_3 + \frac{1}{3}u_5 - \frac{4}{3}u_\lambda\right)(L+1), \\ f_5 &= u_5 + \frac{5\epsilon}{3}\left(u_5 - 2u_\lambda\right)(L+1). \end{aligned} \tag{2.64}$$

In this form the complete scaling EOS and the above asymmetric RG EOS can be compared term by term.

2.4 Consistency of complete scaling at $O(\epsilon)$

Nicoll has shown that the existence of the $1-\alpha$ term associated with revised scaling in $\overline{\Delta\rho}$ follows from a RG treatment of fluid asymmetry, *i.e.* from Eq. 2.63. We will now illustrate his proof to $O(\epsilon)$. The concept is to find a linear combination of the asymmetric operators that reproduces the effect of revised scaling. The portion of the EOS due to revised scaling is found by setting $a = c = 0$ in Eq. 2.33, which yields

$$\begin{aligned} \Delta\tilde{f} = \Psi|_0 &+ b\left\{-\frac{(\Delta T)^2}{g}\Delta\rho + \frac{1}{3!}\left(2 + \frac{1}{9}\epsilon\,(L+1)\right)\Delta T(\Delta\rho)^3\right. \\ &+ \left.\frac{g}{5!}\left(10 + \frac{20}{3}\epsilon\,(L+1)\right)(\Delta\rho)^5\right\}, \end{aligned} \tag{2.65}$$

where $\Psi|_0$ is the Ising-type Helmholtz energy introduced in Eq. 2.23. Consistency with the mean-field EOS, Eq. 1.45, which is found by taking $\epsilon \rightarrow 0$, requires $u_1 = -b$, $u_3 = 2b$ and $u_5 = 10b$. The terms of $O(\epsilon)$ are also matched to those in Eq. 2.64 if $u_\lambda = 3b$. We can now define a revised scaling operator,

$$O_b = -O_1 + 2O_3 + 10O_5 + 3O_\lambda. \tag{2.66}$$

The effects of revised scaling can be reproduced by adding bO_b to the Ising Hamiltonian. However, the linear combination O_b does not span the the entire asymmetric LGW Hamiltonian, Eq. 2.48. Three additional linearly-independent operators are required. For these we choose O_1, O_3 and O_5. The asymmetric portion of the Hamiltonian can now be written

$$\mathcal{H}_A = u_1^{eff} O_1 + u_3^{eff} O_3 + u_5^{eff} O_5 + bO_b \tag{2.67}$$

The effective coefficients are selected to reproduce the original asymmetric Hamiltonian. To this end,

$$u_1^{eff} = u_1 + \frac{1}{3}u_\lambda \tag{2.68}$$

$$u_3^{eff} = u_3 - u_\lambda \tag{2.69}$$

$$u_5^{eff} = u_5 - \frac{10}{3}u_\lambda \tag{2.70}$$

$$b = \frac{1}{3}u_\lambda, \tag{2.71}$$

where we have omitted the superscript "0" to simplify the presentation. The total effect of the asymmetric Hamiltonian on the excess density will be the sum of the effects of the constituent operators. Therefore, we also need to know the individual effects of O_1, O_3 and O_5.

The coefficient u_1 does not enter the fluctuation operator, Eq. 2.56. Therefore, O_1 only makes a mean-field contribution to the Helmholtz energy and does not effect the excess density. For this reason, this operator can typically be ignored. Here we keep it for consistency.

The operator O_3 can be removed from the Hamiltonian without altering the other terms at leading order, by making the transformation $\phi \to \phi - (u_3^0/g_0)\Delta T_0$. Below the critical point, the effects of this term on the density can be restored by applying the reverse transformation, *i.e.*, $\Delta\rho \to \Delta\rho - (\nu_3/g)\Delta T$. This result can also be found by applying, the mean-field formula for the excess density, Eq 2.34, to the O_3 portion of the Helmholtz energy,

$$\Delta\tilde{f} \sim u_3 \frac{1}{3!}\left(1 + \frac{\epsilon}{2}(L+1)\right)\Delta T(\Delta\rho)^3. \tag{2.72}$$

The implications of adding O_5 do not have a unique interpretation in the ϵ-expansion. The equation of state generated solely from the insertion of O_5 is,

$$\begin{aligned}\Delta\tilde{f} = \Psi|_0 + u_5 \Bigg\{ &\frac{1}{3!}\left(\frac{\epsilon}{6}(L+1)\right)\Delta T(\Delta\rho)^3 \\ &+ \frac{g}{5!}\left(1 + \frac{5}{3}\epsilon(L+1)\right)(\Delta\rho)^5\Bigg\}.\end{aligned} \tag{2.73}$$

The quintic term in Eq. 2.73 is responsible for the exponent θ_5. The cubic term requires some interpretation. Without a leading mean-field contribution, the cubic term is classified by Nicoll as a "non-scaling" term. When, as here, the ϵ-expansion is performed only to a limited, fixed order, a so-called non-scaling contribution does not have a unique interpretation as a power law. More generally, as is well known, it is necessary to carry the expansion to higher orders in ϵ to resolve such

ambiguities. This same issue is encountered when interpreting the entropy. Nicoll chose to interpret the cubic term as producing the same temperature dependence as the scaling contribution from the quintic term by letting,

$$u_5 \frac{\epsilon}{6}(L+1) = \frac{1}{5}u_5\left(1 + \frac{5\epsilon}{6}(L+1)\right) - \frac{1}{5}u_5. \tag{2.74}$$

This interpretation yields an excess density that varies as

$$\overline{\Delta\rho} \sim -\frac{3}{5}u_5|\Delta T|^{\beta+\theta_5} + \frac{1}{5}u_5\left(|\Delta T|^{\beta+\theta_5} - |\Delta T|\right). \tag{2.75}$$

The final term was described as a "shifting diameter-background" that crosses over from $\overline{\Delta\rho} \sim -\frac{3}{5}\nu_5|\Delta T|$ in mean-field to $\overline{\Delta\rho} \sim -\frac{1}{5}\nu_5|\Delta T|$ in the critical region [24].

The total excess density produced by Eq. 2.67 is

$$\overline{\Delta\rho} = b\Delta s + \frac{u_3^{eff}}{g}|\Delta T| - \frac{3}{5}u_5^{eff}|\Delta T|^{\beta+\theta_5} + \frac{1}{5}u_5^{eff}\left(|\Delta T|^{\beta+\theta_5} - |\Delta T|\right). \tag{2.76}$$

In the mean-field EOS ($\epsilon \to 0$) all dependence on u_λ cancels, and the expected result is recovered. Thus Nicoll's treatment of the asymmetric Hamiltonian produces an excess density with a leading $1-\alpha$ term, which disappears if $u_\lambda = 0$, and a higher order $\beta + \theta_5$, in addition to the linear term.

The non-scaling term in Eq. 2.73 can also be interpreted as producing singular contributions to the diameter. Instead of forcing this term to match the behavior of the quintic term, it can be treated independently. For instance, by letting

$$u_5\left(\frac{\epsilon}{6}L\right) = u_5\left(1 + \frac{\epsilon}{6}L\right) - u_5, \tag{2.77}$$

we find

$$\overline{\Delta\rho} \sim -\frac{3}{5}u_5|\Delta T|^{\beta+\theta_5} + u_5\left(|\Delta T|^{1-\alpha} - |\Delta T|^{2\beta}\right). \tag{2.78}$$

Both a 2β and a $1-\alpha$ exponent appear in the excess density as a result of this interpretation. Even though the physical implications are markedly different, this result, when expanded to first order in ϵ, is identical to Eq. 2.75. Without a guiding principle there is no way, within the current approach, to know which, if either, is the more physically meaningful interpretation. As noted above, it will be necessary to proceed to higher order in the ϵ-expansion to clarify this issue more fully.

The methodology of the preceding paragraphs can also be applied to complete scaling. The key is to search for linear combinations of the asymmetric operators that will reproduce the entire complete scaling EOS. When $b = c = 0$, the complete scaling EOS, Eq. 2.33, can be reproduced for $u_1 = -(1/2)\hat{a}$, $u_3 = -3\hat{a}$, $u_5 = -15\hat{a}$, and $u_\lambda = -(21/4)\hat{a}$, so that adding the operator O_a, defined by

$$O_a = \frac{1}{2}O_1 - 3O_3 - 15O_5 - \frac{21}{4}O_\lambda, \tag{2.79}$$

to $\mathcal{H}_I$ has the same effect as the pressure mixing in Eq. 2.4. Similarly, for $a = b = 0$, we find

$$O_c = O_1 - O_3. \tag{2.80}$$

Therefore the entire asymmetric hamiltonian can represented as

$$\mathcal{H}_A = u_1^{eff}O_1 + aO_a + bO_b + cO_c. \tag{2.81}$$

The operator O_1 creates an addition to the background chemical potential that does not enter into physically interesting quantities. In order to make the mapping between the complete scaling EOS and the RG EOS exact, we will treat u_1 as a free parameter and use it to set $u_1^{eff} = 0$. Alternatively, O_1 can be matched by adding

an additional term $\sim (\Delta T)^2$ to h in the complete scaling transforms, Eq. 2.4. However, in the present $O(\epsilon)$ approach, this creates an unnecessary complication. The connection to the original form of the Hamiltonian is given by

$$\begin{aligned} u_3 &= 3b - 3\hat{a} - \hat{c}, \\ u_5 &= 10b - 15\hat{a}, \\ u_\lambda &= 3b - \frac{21}{4}\hat{a}, \end{aligned} \tag{2.82}$$

where $\hat{a} = a(1 + \epsilon/12)$ and $\hat{c} = gc$ were introduced in Eqs. 2.31 and 2.32. The inverse relations are

$$\begin{aligned} \hat{a} &= \frac{2}{5}u_5 - \frac{4}{3}u_\lambda, \\ b &= \frac{7}{10}u_5 - 2u_\lambda, \\ \hat{c} &= u_3 - \frac{1}{5}u_5. \end{aligned} \tag{2.83}$$

These results are different from the relationships found by Wang and Anisimov, Eq. 1.55, which do not include u_λ. Their results correspond to the special case $\hat{c} - b = 0$. This condition can be used to eliminate u_λ from the expressions for a and b, thereby reproducing the Eq. 1.55. The definition of $c = \hat{c}/g$ carries an awkward factor of $1/g$, which corresponds to the background heat capacity $B_{\rm cr}$, so we can write $c = \hat{c}B_{\rm cr}$, which is more physically meaningful. The definition of $\hat{a} = a(1 + \epsilon/12)$ carries a non-universal factor, which makes the relationship between a and the coefficients u_5 and u_λ system dependent. In what follows, we will neglect this non-universal factor by assuming that $\hat{a} \simeq a$.

In deriving the complete scaling EOS, we chose $\Psi_0(\Delta T) = -(\Delta T)^2/2g$ in Eq.

2.23. Other authors have taken $\Psi_0 = 0$, so that the fluctuation-induced background contribution to the entropy $B_{\rm cr}\Delta T$, which was introduced in Eq. 1.5 and disucssed below Eq. 1.37, is retained. This second choice leads the excess density,

$$\overline{\Delta\rho} = a^*(B_0)^2|\Delta T|^{2\beta} - b^*\frac{A_0^-}{1-\alpha}|\Delta T|^{1-\alpha} + (b^*B_{\rm cr} + c^*)\,|\Delta T|. \tag{2.84}$$

This expression appears to contradict Eq. 2.40, which predicts a slightly different amplitude for the linear term. The apparent contradiction is resolved by changing the mapping between the parameters in the complete scaling EOS and the coefficients in the asymmetric RG EOS. For a Helmholtz energy with $\Psi_0 = 0$, the choice of parameters that maps complete scaling onto the asymmetric RG EOS is

$$\begin{aligned} a^* &= a \\ b^* &= b \\ c^* &= \frac{1}{g}(u_3 - \frac{9}{10}u_5 + 2u_\lambda). \end{aligned} \tag{2.85}$$

where a superscript has been added to distinguish these parameters from those in Eq. 2.83. Only the value of c^* differs from the ones presented in Eq. 2.83. The critical background at this order is $B_{\rm cr} = 1/g$, hence,

$$c = b^*B_{\rm cr} + c^* = \frac{1}{g}(u_3 - \frac{1}{5}u_5). \tag{2.86}$$

Both approaches predict the same form for the excess density, in terms of the physically meaningful coefficients, u_i. The Wang and Anisimov relations for the complete scaling parameters, Eq. 1.55, correspond to the special case $c^* = 0$.

2.5 Comparison with experiment

Values for the complete scaling parameters a, b and $\hat{c}$, can be found by fitting experimental excess density data with Eq. 2.40. The parameters can then be used to determine the coefficients of the asymmetric Hamiltonian, u_5, u_λ, and u_3, through Eq. 2.83. Wang and Anisimov have previously done this for a number of substances by assuming $c - b = 0$ or equivalently, $c^* = 0$ [28]. We have fit coexistence curve data from eight substances: hydrogen deuteride (HD) [31], neon (Ne) [31], nitrogen (N_2) [31], ethene (C_2H_4) [31], ethane (C_2H_6) [31], sulfur hexafluoride (SF_6) [30], freon-113 ($C_2Cl_3F_3$) [52], and heptane (C_7H_{16}) [53]. In order to determine B_0, the density difference was fit to

$$\Delta\rho_0 = B_0|\Delta T|^\beta \left(1 + B_1|\Delta T|^\Delta\right), \tag{2.87}$$

over the reduced temperature range $10^{-4} < \Delta T < 10^{-2}$. This range was chosen because data points closer to the critical point are susceptible to systematic error, and points further from the critical point could be affected by higher-order terms. The values of the exponents were set at $\beta = 0.326$ and $\Delta = 0.5$, and B_0 and B_1 were treated as free parameters. The values obtained for B_0 are listed in Table 2.1. The form of excess density that was fit to is given by

$$\overline{\Delta\rho} = D_{2\beta}|\Delta T|^{2\beta} + D_{1-\alpha}|\Delta T|^{1-\alpha} + D_1|\Delta T|. \tag{2.88}$$

It is difficult to get a meaningful fit from this equation if all three amplitudes are left free. This is because the $|\Delta T|^{1-\alpha} = |\Delta T|^{0.89}$ and $|\Delta T|$ terms are highly correlated. If the value of D_1 is held fixed, the fit value for $D_{1-\alpha}$ is of the same order but

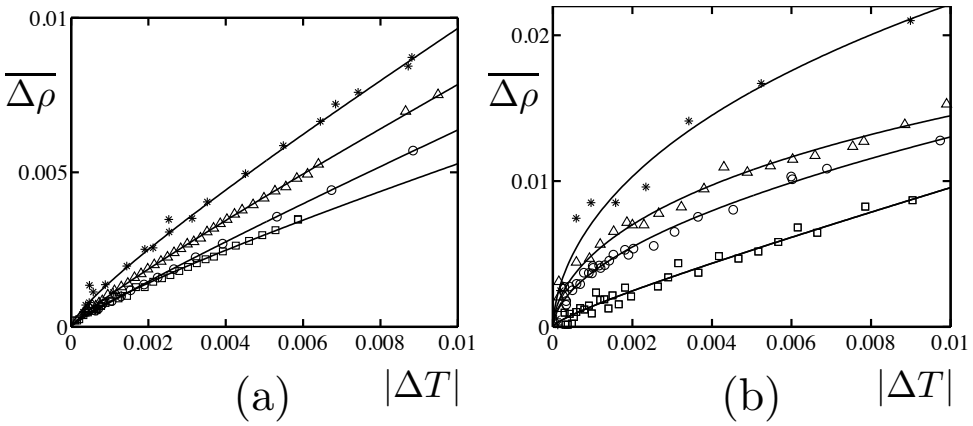

Figure 2.2: Liquid-vapor excess densities near the critical point. Experimental data are shown by symbols. For (a) [31]: □-HD, ◯-Ne, △-N_2, and ∗-C_2H_4. For (b): □-C_2H_6 [31], ◯-SF_6 [30], △-$C_2Cl_3F_3$ [52], and ∗-C_7H_{16} [53]. Curves correspond to fits to Eq. 2.88

of opposite sign. If D_1 is varied over a range of positive and negative values, the standard deviations of the fits only exhibit a very shallow minima that cannot be used to determine the optimal value. In order to obtain a stable fit, one may make a physically reasonable approximation for the value of D_1 and then fit for $D_{2\beta}$ and $D_{1-\alpha}$.

Wang and Anisimov have introduced the normalized interaction volume $v_{\rm int} = v_{\rm c}/(2\xi_0^+)^3$, where $v_{\rm c} = 1/\rho_{\rm c}$, to characterize the asymmetry of a system [28]. Values of $v_{\rm int}$, taken from their paper, are listed in Table 2.1. Helium-3 has a nearly symmetric coexistence curve, and the interaction volume is $v_{\rm int} \simeq 2.5$ [54]. We can take the Helium-3 values as the zero-point for the rectilinear portion of the diameter, and then allow D_1 to increase as a function of $v_{\rm int}$. Specifically, we will take

$$D_1 = 0.5(v_{\rm int} - 2.5). \tag{2.89}$$

The prefactor 0.5 was chosen so that the resulting mixing parameters will be of

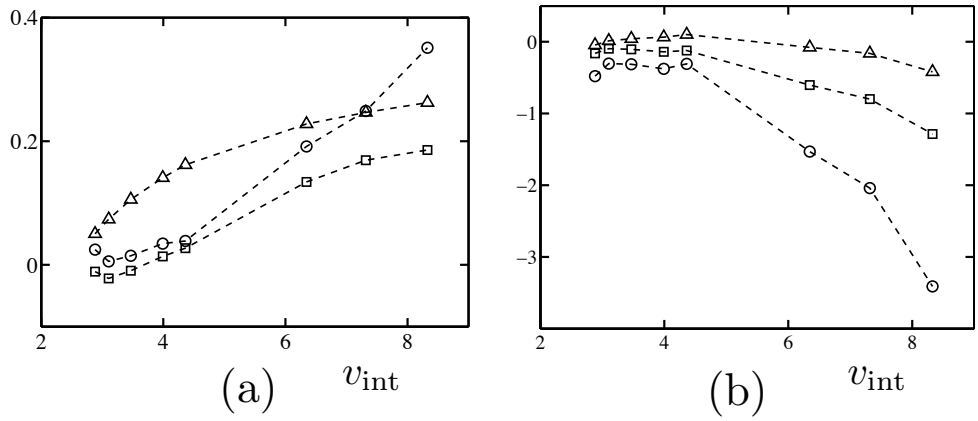

Figure 2.3: Complete scaling mixing-parameters (a) and asymmetry coefficients (b) plotted versus the interaction volume $v_{\rm int}$. Dashed lines have been added to guide the eye. For (a): a-◯, b-□, $\hat{c}$-△. For (b): u_5-◯, u_λ-□, u_3-△

the same order of magnitude in highly asymmetric systems. We could also impose an additional condition that the excess density not exhibit a "wiggle", specifically that the diameter be convex down, *i.e.* $d^2\overline{\Delta\rho}/d|\Delta T|^2 < 0$. This condition can be reexpressed as

$$\frac{D_{2\beta}}{D_{1-\alpha}} > \frac{\alpha(1-\alpha)}{2\beta(1-2\beta)}|\Delta T|^{1-\alpha-2\beta} \simeq 0.14. \tag{2.90}$$

The final value in this equation in based on $\Delta T = 0.01$. This will be satisfied if the mixing parameters are positive.

The excess density data was fit to Eq. 2.88 over the reduced temperature range $10^{-4} < \Delta T < 10^{-2}$, with D_1 held fixed by Eq. 2.89 . The results of these fits are presented in Fig. 2.2. The conversions from the fit amplitudes to the actual mixing-parameters are made via

$$D_{2\beta} = a(B_0)^2,\ D_{1-\alpha} = -bA_0^-/(1-\alpha),\ \text{and}\ D_1 = \hat{c}B_{\rm cr}. \tag{2.91}$$

The measured, or interpolated, values of A_0^-, taken from [28], are included in Table

2.1. The background heat capacity can be roughly estimated as $B_{cr} \simeq A_0^+ = 0.55 A_0^-$. The values of a, b, and $\hat{c}$ and u_5, u_λ, and u_3 obtained from the fits are listed in Table 2.2 and plotted versus $v_{\rm I}$ in Fig. 2.3. The values for a and b determined for the three most symmetric substances, HD, Ne, and N_2, are scattered around zero. Given the quality of data, we do not read any special significance into the negative values for b, which might correspond to an over-estimation of $\hat{c}$. Therefore we conclude that the mixing parameters a, b, and $\hat{c}$ should generally be taken to be positive. The Hamiltonian coefficients are negative except for some minor scattering for low asymmetry systems that again should not be considered as physically meaningful. Additionally they generally follow the ordering $|u_5| > |u_\lambda| > |u_3|$. The relative size of the asymmetry coefficients can be bounded from the positivity of the mixing-parameters. $a > 0$ implies, for negative u_5 and u_λ, that $|u_5| < (10/3)|u_\lambda|$, and $\hat{c} > 0$ implies that $|u_5| > 5|u_3|$. The signs of the mixing-parameters and asymmetry coefficients, and their relative orderings are robust against variations of the fixed form of D_1.

2.6 Summary and Conclusions

In Sec. 2.2, we argued that the simplified complete scaling transformations, Eq. 1.51, need to be modified by two additional non-linear terms. The resulting transformations, presented in Eq. 2.4, compactly account for all leading sources of asymmetry. The form of the density predicted by the modified transformations is given in Eq. 2.5. The equation of state implied by the complete scaling transforma-

	T_c (K)	ρ_c (g/cm^3)	A_0^- (J/mol K)	B_0	v_{int}
HD	35.957	0.0481	(65)	1.30	2.88
Ne	44.479	0.484	(70)	1.44	3.10
N_2	126.214	0.314	78	1.52	3.47
C_2H_4	282.377	0.215	(90)	1.60	3.99
C_2H_6	305.363	0.206	98	1.6	4.36
SF_6	318.707	0.733	143	1.71	6.35
$C_2Cl_3F_3$	486.968	0.567	(165)	1.80	7.32
C_7H_{16}	539.860	0.234	188	1.78	8.33

Table 2.1: Critical parameters and amplitudes. The values of T_c and ρ_c are from [31] for HD, Ne, N_2, C_2H_4, and C_2H_6, from [30] for SF_6, from [52] for $C_2Cl_3F_3$, and [53] for C_7H_{16}. The values of A_0^- and v_{int} are taken from [28]. The amplitudes B_0 were found from fits to Eq. 2.87

	a	b	$\hat{c}$	u_5	u_λ	u_3
HD	0.025	-0.011	0.050	-0.480	-0.162	-0.046
Ne	0.006	-0.022	0.074	-0.305	-0.096	0.013
N_2	0.015	-0.010	0.106	-0.314	-0.105	0.043
C_2H_4	0.034	0.014	0.141	-0.378	-0.139	0.065
C_2H_6	0.039	0.027	0.162	-0.307	-0.121	0.100
SF_6	0.192	0.134	0.228	-1.532	-0.603	-0.078
$C_2Cl_3F_3$	0.249	0.169	0.247	-2.04	-0.799	-0.162
C_7H_{16}	0.351	0.186	0.262	-3.411	-1.287	-0.420

Table 2.2: Mixing parameters and asymmetry coefficients based on fits to Eq. 2.88. The mixing parameters a, b, and $\hat{c}$ were found from Eq. 2.91. The asymmetry coefficients were found from Eq. 2.83.

tions was then derived for both the pressure, Eq. 2.9 , and the Helmholtz energy, Eq. 2.17. The complete scaling Helmholtz energy was explicitly calculated to $O(\epsilon)$ in Eq. 2.29, and it was shown that all predictions of complete scaling can be consistently derived to $O(\epsilon)$ from this EOS. Next, in Sec. 2.3, the asymmetric "RG EOS", Eq. 2.63, based on a RG analysis of a general asymmetric LGW Hamiltonian, Eq. 2.48, was calculated in the one-loop approximation. This result matches Nicoll's previous work [24]. A careful analysis of the terms in the asymmetric RG EOS showed that the interpretation of the EOS leading to the asymmetric correction to scaling exponent θ_5 is not unique, and that the EOS can be interpreted as producing 2β and $1-\alpha$ contributions to the excess density. The principle result of this chapter, a demonstration of the consistency of complete scaling to $O(\epsilon)$, was presented in Sec. 2.4. In this section, the results of the two preceding sections were combined to show that the complete scaling EOS and the asymmetric RG EOS are identical at $O(\epsilon)$ for an appropriate choice of the field-mixing parameters. This result was shown to be robust when the fluctuation-induced background contribution to the entropy density is included in the scheme, *cf.* Eq. 2.84 and the surrounding material. We have fit experimental excess density data to Eq. 2.88 in order to determine the complete scaling mixing parameters a, b, and c and the asymmetry coefficients u_5, u_λ, and u_3. The mixing parameters are found to be positive for the highly asymmetric systems, and the asymmetry coefficients are found to be negative, or close to zero for systems with low asymmetry, and to obey the ordering $|u_5| > |u_\lambda| > |u_3|$ as seen in Fig. 2.3.

Chapter 3

Complete scaling for inhomogeneous fluids

3.1 Introduction

When liquid and vapor coexist in equilibrium, the interface between them plays a role in the thermodynamics. The interfacial Helmholtz energy per unit area of interface is known as the interfacial, or surface, tension, and is denoted by σ. Like many thermodynamic properties, the interfacial tension exhibits universal, non-analytic behavior in the vicinity of a critical point [55]. In this chapter we investigate interfacial critical phenomena in asymmetric fluid systems.

As the liquid-vapor critical point is approached from below the critical point along the critical isochore, the interface separating the two phases becomes more diffuse and the density difference $\Delta\rho_0$ goes to zero. In the critical region, the smooth variation of the density across the interfacial region can be described by a continuous interfacial profile. This profile is an object of principal interest because it can be used to derive the surface tension. The interfacial profile is determined by finding the density configuration that minimizes the Helmholtz energy of the system for $t < 0$. The same is true for the magnetization in an Ising-type system. For the mean-field Ising EOS (Eq. 1.37) this implies

$$\left(\frac{\delta\Psi(m,t,\nabla m)}{\delta m}\right)_t = -\nabla^2 m + tm + \frac{g}{6}m^3 = 0, \tag{3.1}$$

where we have defined the functional derivative by

$$\frac{\delta}{\delta m} = \frac{\partial}{\partial m} - \nabla \cdot \frac{\partial}{\partial(\nabla m)}. \tag{3.2}$$

Here and throughout, we will take the interface to lie in the x-y plane, so that the magnetization (or density) varies along the z-direction. If the mean-field magnetization, given by Eq. 1.39, is denoted by m_0, then the solution of the differential equation can be written as,

$$m(z) = m_0 \tanh(\hat{z}). \tag{3.3}$$

where we have defined

$$\hat{z} = \frac{z}{2\xi}, \tag{3.4}$$

where ξ, in this context, is the mean-field correlation length, given by Eq. 1.43. This result is originally due to van der Waals [56, 57]. The constant of integration has been set to zero to locate the center of the interface at $z = 0$, *i.e.* $m(z = 0) = 0$. Equation 3.3 shows that the interfacial thickness is controlled by the only relevant length scale in the critical region, the correlation length. For symmetric coexistence, the surface tension is given by,

$$\sigma = \int dz \left(\Psi[m(z)] - \Psi[m_0]\right). \tag{3.5}$$

For the mean-field EOS, an equivalent expression is

$$\sigma = \int dz |\nabla m|^2, \tag{3.6}$$

which, when combined with Eq 3.3, yields

$$\sigma = \frac{2(m_0)^2}{3\xi} = \frac{4\sqrt{2}}{g}|t|^{3/2}. \tag{3.7}$$

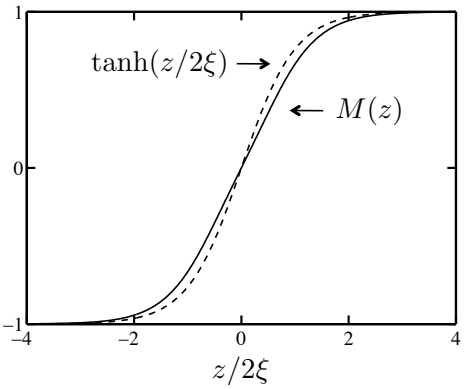

Figure 3.1: Symmetric interfacial profile functions found in Eqs. 3.3 and 3.9.

Ohta and Kawasaki [58], and Rudnick and Jasnow [59], have extended this approach by calculating the interfacial profile to $O(\epsilon)$ for the Ising-type EOS derived in Appendix A. They found

$$m(z) = B_0|t|^\beta M(z), \tag{3.8}$$

where the profile function is

$$M(z) = \tanh(z/2\xi)\left[1 - \frac{\pi\epsilon}{6\sqrt{3}}\mathrm{sech}^2(z/2\xi)\right]. \tag{3.9}$$

The correlation length ξ appearing in this expression is the $O(\epsilon)$ correlation length. The profile for the function $M(z)$ and the mean-field profile are plotted in Fig. 3.1 for comparison. The critical fluctuations tend to smooth out the shape of the profile. The value of the interfacial tension for Eq. 3.8 is $\sigma = C_0(B_0|t|^\beta)^2/\xi \sim |t|^{2\beta+\nu}$. This matches the predictions, based on scaling arguments, of Fisk and Widom [60]. The value of the universal constant C_0 differs slightly depending on whether Eq. 3.5 or the approximation Eq. 3.6 is used as a result of non-local contributions to the Helmholtz energy.

The interfacial profile presented in Eq. 3.8 was derived in an expansion around $d = 4$. By taking $\epsilon \to 1$, one can extrapolate the result to $d = 3$. Although this is the typical approach for interpreting the ϵ-expansion, it skirts the issue of capillary waves [61], which are known to be relevant for $d = 3$. Calculating the magnetization profile in an epsilon expansion around $d = 3$, Jasnow and Rudnick found that capillary-wave like fluctuations destroy the profile in the absence of an external "pinning" field, such as gravity for a fluid [62, 63]. In their treatment, the gravitational field makes a small non-universal contribution to the profile. In spite of its defficiencies, the value of the surface tension calculated from Eq. 3.8 is in good agreement with experimental measurements [58].

When the interface between coexisting fluids is curved, and not planar, the value of the interfacial tension is modified. This effect was first investigated by Tolman [64], who considered a spherical droplet of liquid, of radius R, surrounded by vapor. If the reduced pressures of the liquid (+) and vapor (−) phases are denoted by $\Delta P^{\pm}$, then the Laplace equation can be written,

$$\Delta P^{+} - \Delta P^{-} = \frac{2\sigma}{R}. \tag{3.10}$$

Based on this equation, Tolman found the surface tension of the curved interface, for large R, to be

$$\sigma\left(R\right) = \sigma_{\infty}\left(1 - \frac{2\delta_{\mathrm{T}}}{R} + \cdots\right), \tag{3.11}$$

where σ_{∞} is the planar surface tension while δ_{T}, the coefficient of the first curvature correction, is known as Tolman's length. The sign of δ_{T} changes for a bubble of vapor, but the magnitude remains the same. Most significantly, Tolman's length is

zero for symmetric systems [65].

In order to investigate the near-critical properties of Tolman's length, Fisher (M. P. A.) and Wortis calculated the interfacial profile for an asymmetric EOS in the mean-field approximation [65]. The asymmetric mean-field EOS they used is very similar to that introduced in Eq. 1.45. To incorporate the energetic contributions of the inhomogeneities they included the square gradient term, but explicitly assumed there is not an asymmetric gradient term, *i.e.*, $u_\lambda = 0$. For a fluid system, the equilibrium density profile minimizes the excess pressure [61]. For a planar profile, this implies

$$\frac{\delta}{\delta\hat{\rho}}(\Delta f - \hat{\mu}_{\rm cxc}\Delta\rho) = -\nabla^2\hat{\rho} + \frac{\partial\hat{f}}{\partial\hat{\rho}} - \hat{\mu}_{\rm cxc} = 0, \tag{3.12}$$

where Δf is given by Eq. 1.45 and $\mu_{\rm cxc}$ is given by Eq. 1.47. By solving this differential equation, one finds

$$\Delta\rho = \Delta\rho_0 \tanh(\hat{z}) + \frac{u_3}{6}(\Delta\rho_0)^2 - \frac{u_5}{10}(\Delta\rho_0)^2\left[\tanh^2(\hat{z}) - \frac{\ln\left(\cosh(\,\hat{z})\right)}{\cosh^2(\hat{z})}\right]. \tag{3.13}$$

where $\hat{z}$ is given by Eq. 3.4. This result reproduces Eq. 1.46 for $\hat{z} \to \pm\infty$.

By expanding the surface tension in inverse powers of the curvature, Fisher and Wortis have also found an expression relating Tolman's length to the *planar* interfacial profile, namely,

$$\delta_{\rm T} = \frac{\int_{-\infty}^{\infty} dz\ z\left(\partial_z\rho\right)^2}{\int_{-\infty}^{\infty} dz\ \left(\partial_z\rho\right)^2} - \frac{\int_{-\infty}^{\infty} dz\ z\partial_z\rho}{\int_{-\infty}^{\infty} dz\ \partial_z\rho}. \tag{3.14}$$

When combined with the profile, Eq. 3.13, this expression produces

$$\delta_{\rm T} = \frac{1}{12}u_5\Delta\rho_0\xi = \frac{1}{4}\frac{u_5}{\sqrt{3g}}. \tag{3.15}$$

The mean-field Tolman's length is proportional to the asymmetry and independent of temperature. The coefficient u_5 is expected to be negative, as is the case for the van der Waal's EOS [65] so that the mean-field Tolman's length is negative for a liquid droplet, and the surface tension is slightly greater than expected from a planar interface. A negative Tolman's length has been confirmed by other mean-field calculations [66], and agrees with the thermodynamic expression derived by Blokhuis and Kuipers [67]. When fluctuations are included, $\beta \neq \nu$, and Tolman's length is expected to depend on temperature, and in fact diverge at the critical point [68]. Anisimov [69] has, via scaling arguments, predicted the near-critical Tolman's length of a droplet to vary as

$$\frac{\delta_{\mathrm{T}}}{2\xi} \sim -\frac{\overline{\Delta\rho}}{\Delta\rho_0}, \tag{3.16}$$

where $\Delta\rho_0$ and $\overline{\Delta\rho}$ were defined in Eqs. 1.27 and 1.28. Equivalently, this can be written

$$\delta_{\mathrm{T}} \sim -\left[\frac{3}{2}a|\Delta T|^{\beta-\nu} - 2b\frac{\beta}{\Gamma_0^-}|\Delta T|^{1-\alpha-\beta-\nu}\right] B_0\xi_0^-. \tag{3.17}$$

Both terms diverge at the critical point, but the leading term diverges much more strongly since $\beta - \nu \simeq -0.304$, where as $1 - \alpha - \beta - \nu \simeq -0.065$. Some older molecular dynamic simulations found Tolman's length to be positive [70, 71, 72]. However, more recent simulations have tried to correct for some of the deficiencies of previous simulations and have found a negative Tolman's legnth in agreement with theoretical predictions [73, 74, 75].

In this chapter, we investigate the behavior of the interfacial profile and Tolman's length near the critical point for asymmetric fluids. Complete scaling is the

theory of asymmetric fluid criticality, but we have so far only applied it to bulk systems. After briefly reviewing the thermodynamics of non-uniform systems in Sec. 3.2 , we extend complete scaling to inhomogeneous systems in Sec. 3.3. This theory is then applied to calculate the full asymmetric interfacial profile based on the symmetric $O(\epsilon)$ profile, Eq. 3.8. In complete scaling, the density depends on both the magnetization and the entropy. Hence the density profile will also depend on the entropy profile. In Sec. 3.5 we take a brief detour to derive the $O(\epsilon)$ entropy profile and discuss some of it implications. Finally, on the basis of the density profile, Tolman's length is calculated in Sec. 3.6 and a brief summary of this chapter's findings is given in Sec. 3.7.

3.2 Thermodynamics of non-uniform systems

As shown by Hart [76], and elaborated by Cahn [77], the effects of mesocopic inhomogeneities can be consistently incorporated into a thermodynamic description of fluids by treating the local density gradient $\nabla\rho$ and the thermodynamic field $\mathbf{w}$, which is conjugate to the density gradient, as additional variables. This treatment assumes that all thermodynamic functions depend smoothly on the spatial coordinates. The field $\mathbf{w}$ is, by definition, related to the Helmholtz energy through

$$\mathbf{w} = \left(\frac{\partial f}{\partial \nabla\rho}\right)_{\rho,T}. \tag{3.18}$$

The Helmholtz energy can be divided into two parts by isolating the $\nabla\rho$ dependence,

$$f(\rho, T, \nabla\rho) = f_0(\rho, T) + \frac{1}{2} f_1(\rho, T, \nabla\rho)|\nabla\rho|^2. \tag{3.19}$$

Here, and in what follows, the gradient-independent portion of a thermodynamic function is denoted by a subscript 0. The division in Eq. 3.19 assumes that the Helmholtz energy is analytic in the density gradient. Near the critical point this is not the case. The deviations from analyticity are characterized by the exponent η. In the first ϵ-expansion, on which much of the following work is based, $\eta = 0$ exactly. At higher orders in ϵ, η is non-zero but sufficiently small - for $d = 3$ spatial dimensions $\eta \simeq \epsilon^2/54$ - that neglecting it may constitute a reasonable approximation. The asymmetric gradient contribution will inherit this assumed analyticity. For the remainder of this work, we assume that f_1 in Eq. 3.19 depends only on ρ. The gradient ordering field $\mathbf{w}$ is then related to the density gradient by

$$\mathbf{w} = f_1 \nabla \rho. \tag{3.20}$$

In the vicinity of the critical point, f_1 can be expanded as

$$f_1 \simeq (\xi_0^+)^2 [1 + (2/3) u_\lambda \Delta\rho], \tag{3.21}$$

where the omitted higher order terms will not enter into our discussion. The factor of 2/3 has been included to match the definition of u_λ as discussed below Eq. 2.48. Convenient dimensionless quantities are defined by

$$\nabla\hat{\rho} = (\xi_0^+ \nabla\rho)/\rho_c \;\text{ and }\; \hat{\mathbf{w}} = \mathbf{w}/(\xi_0^+ T_c). \tag{3.22}$$

The mean-field Helmholtz energy near the critical point can therefore be written as

$$\Delta f = \Delta f_0 + \frac{1}{2}(1 + \frac{2}{3} u_\lambda \Delta\rho) |\nabla\hat{\rho}|^2. \tag{3.23}$$

The effect of the asymmetric gradient term can be understood as making an asymmetric contribution to the correlation length. In analogy with the symmetric

result found in the $\eta = 0$ approximation, *cf.* Eq. 1.43, Eq. 3.23 suggests that the asymmetric correlation length behaves roughly as

$$\xi_a^2 \sim f_1 \chi_T \sim (1 \pm \frac{2}{3} u_\lambda B_0 |\Delta T|^\beta) \chi_T, \tag{3.24}$$

where χ_T is the bulk asymmetric susceptibility. The bulk isothermal susceptibility also contains an asymmetric correction, which could make it difficult to distinguish the two sources of correlation length asymmetry. However, if both the isothermal susceptibility and correlation length were measured in the bulk portions of the coexisting phases, the coefficient in front of the asymmetric gradient might be estimated independently.

In addition to the definition of the field $\mathbf{w}$ presented in Eq. 3.18, Hart also defines the entropy and a chemical potential by

$$s = -\left(\frac{\partial f}{\partial T}\right)_{\rho, \nabla\rho}, \ \mu = \left(\frac{\partial f}{\partial \rho}\right)_{T, \nabla\rho}, \tag{3.25}$$

which imply that

$$df = -s dT + \mu d\rho + \mathbf{w} \cdot d(\nabla\rho). \tag{3.26}$$

This definition of μ differs from the "standard" definition of the chemical potential. Specifically, in equilibrium, μ may not be uniform for an inhomogeneous system. Alternatively, a total chemical potential, which also differs from the standard defintion, can be defined via a functional derivative, namely,

$$\mu_{tot} = \frac{\delta f}{\delta \rho} = \frac{\partial f}{\partial \rho} - \nabla \cdot \frac{\partial f}{\partial \nabla \rho}, \tag{3.27}$$

so that $df = -s dT + \mu_{tot} \delta\rho$. Hence, $\mathbf{w}$ can be understood as the portion of the total chemical potential associated with spatial variations of the density.

Hart also defines a pressure P via the Legendre transformation

$$P = (\mu\rho + \mathbf{w} \cdot \nabla\rho) - f. \tag{3.28}$$

Like the definition of the chemical potential μ in Eq. 3.25, this definition of P differs from the "standard" definition of the pressure, in that P may not be uniform in an inhomogeneous system. The above Legendre tranformation leads to the relation

$$dP = \rho d\mu + sdT + \nabla\rho \cdot d\mathbf{w}. \tag{3.29}$$

This provides an extension of the Gibbs-Duhem relation to inhomogeneous systems. The form of Eq. 3.29 indeed prompts us to treat $\nabla\rho$ as a density variable and $\mathbf{w}$ as a field variable, in the nomenclature of Griffiths and Wheeler [10], in spite of the fact that both $\nabla\rho$ and $\mathbf{w}$ vanish in bulk homogeneous phases. The density-like properties are found from the following thermodynamic relations,

$$\rho = \left(\frac{\partial P}{\partial \mu}\right)_{T,\mathbf{w}}, \; s = \left(\frac{\partial P}{\partial T}\right)_{\mu,\mathbf{w}}, \nabla\rho = \left(\frac{\partial P}{\partial \mathbf{w}}\right)_{\mu,T}. \tag{3.30}$$

Finally we note that for a homogeneous system ($\nabla\rho = 0$) the thermodynamic variables defined in this chapter reduce to their standard definitions.

3.3 Complete scaling for inhomogeneous fluids

In the context of complete scaling we need to discuss symmetric and asymmetric systems simultaneously. For the symmetric Ising-type system, we will use the same "magnetic" notation from the previous chapters. For the symmetric system, we can introduce the magnetization gradient ∇m, which is analogous to $\nabla\hat{\rho}$, as a

new thermodynamic variable. If the Helmholtz energy is assumed to be analytic in ∇m, then it can be expanded as

$$\Psi(m, t, \nabla m) \simeq \Psi_0(m, t) + \frac{1}{2}|\nabla m|^2. \tag{3.31}$$

This equation is the symmetric analog of Eq. 3.19. The assumption of analyticity is equivalent to setting $\eta = 0$. Strictly speaking this is only valid to order $O(\epsilon)$. However, as mentioned in the previous section, η is generally small for $d = 3$ and in first analysis it is reasonable to hope that η does not alter the thermodynamic behavior significantly. This approximation also implies that ∇m may be regarded as thermodynamically conjugate to itself,

$$\nabla m = \left(\frac{\partial \Psi}{\partial \nabla m}\right)_{t,m}. \tag{3.32}$$

If the entropy and the applied field are now defined by

$$s = -\left(\frac{\partial \Psi}{\partial t}\right)_{m,\nabla m}, \; h = \left(\frac{\partial \Psi}{\partial m}\right)_{t,\nabla m}, \tag{3.33}$$

then the differential of the Helmholtz energy can be written

$$d\Psi = -sdt + hdm + \nabla m \cdot d(\nabla m). \tag{3.34}$$

In analogy with Eq. 3.28, and with the same caveats, we can define a density of the "Ising" grand potential $-\Phi$ through the Legendre transformation

$$\Phi = (mh + \nabla m \cdot \nabla m) - \Psi, \tag{3.35}$$

which leads to the relation

$$d\Phi = sdt + mdh + \nabla m \cdot d(\nabla m). \tag{3.36}$$

As in the previous section, the above relations for inhomogeneous systems reduce to the standard definitions in the "homogeneous limit" $\nabla m = 0$.

The complete scaling transformations can be extended to inhomogenous systems if the vector ordering fields ∇m and $\mathbf{w}$ are included in the field mixing. The transformations should remain invariant under spatial inversion. Consequently, the leading contributions from $\hat{\mathbf{w}}$ to the scaling fields t, h, and Φ should be proportional to $|\hat{\mathbf{w}}|^2$, and the leading contribution to ∇m must be proportional to $\hat{\mathbf{w}}$. The extended complete scaling transformations are,

$$h = a_1\Delta\mu + a_2\Delta T + a_3\Delta P + \frac{1}{2}a_4|\hat{\mathbf{w}}|^2\cdots, \tag{3.37}$$

$$t = b_1\Delta T + b_2\Delta\mu + b_3\Delta P + \frac{1}{2}b_4|\hat{\mathbf{w}}|^2\cdots, \tag{3.38}$$

$$\Phi = c_1\Delta P + c_2\Delta\mu + c_3\Delta T + \frac{1}{2}c_4|\hat{\mathbf{w}}|^2\cdots, \tag{3.39}$$

$$\nabla m = d_1\hat{\mathbf{w}} + d_2\Delta T\hat{\mathbf{w}} + d_3\Delta P\hat{\mathbf{w}} + d_4\Delta\mu\hat{\mathbf{w}}\cdots. \tag{3.40}$$

We will now simplify these transformations by retaining only those terms that make a leading asymmetric contribution to the thermodynamics. The explanations of why particular terms can be omitted are similar to those used to justify the "homogeneous" complete scaling transformations in Sec. 2.2. At lowest order, we find that $|\hat{\mathbf{w}}|^2 \sim O(\Delta T^{2-\alpha})$, just like ΔP. Therefore, $|\hat{\mathbf{w}}|^2$ makes an asymmetric contribution to h, but not to t or Φ. The non-linear terms in the relation for ∇m, the smallest of which is $\hat{\mathbf{w}}\Delta T$, all lead to higher order contributions and can be omitted. The

simplified transformations are

$$h = \Delta\mu + a\Delta\tilde{P} + \frac{1}{2}a_\lambda|\hat{\mathbf{w}}|^2, \tag{3.41}$$

$$t = \Delta T + b\Delta\mu, \tag{3.42}$$

$$\Phi = \Delta\tilde{P} + c\Delta T\Delta\mu, \tag{3.43}$$

$$\nabla m = \hat{\mathbf{w}}, \tag{3.44}$$

where a new asymmetry parameter a_λ has been introduced, and where the critical portion of the pressure $\Delta\tilde{P}$ was defined in Eq. 1.24. Applying Eq. 3.30 to Eqs. 3.41-3.44, one obtains

$$\hat{\rho} = \frac{1 + (1-a)m + b\Delta s - ct}{1 - am}, \tag{3.45}$$

$$\nabla\hat{\rho} = \left(\frac{1 + a_\lambda m}{1 - am}\right)\nabla m. \tag{3.46}$$

When expanded to linear order in the asymmetry, these become

$$\Delta\hat{\rho} \simeq m + am^2 + b\Delta s - ct, \tag{3.47}$$

$$\nabla\hat{\rho} \simeq [1 + (a + a_\lambda)m]\,\nabla m. \tag{3.48}$$

Comparing Eq. 3.48 with $\hat{\mathbf{w}} = [1 + (2u_\lambda/3)\Delta\rho]\nabla\hat{\rho}$ (Eq. 3.21), we conclude that

$$a_\lambda = -a - \frac{2}{3}u_\lambda = \frac{2}{3}u_\lambda - \frac{2}{5}u_5, \tag{3.49}$$

where use has been made of Eq. 2.83 for a. Even for $u_\lambda = 0$, gradient mixing is necessary, due to the non-linear dependence of density on magnetization. Eqs. 3.47 and 3.48 do not lead to a unique expression for $\Delta\rho$. This can be seen by taking the gradient of Eq. 3.47, which yields

$$\nabla\hat{\rho} \simeq [1 + 2am]\nabla m + b\nabla s. \tag{3.50}$$

This equation is incompatible with Eq. 3.48. Equations 3.47 and 3.48 can be made compatible if Eq. 3.48 is interpreted as describing a coordinate transformation. The coordinate transformation can be consistently formulated if two different gradients are defined as follows:

$$\nabla\hat{\rho} = \frac{\partial\hat{\rho}(\mathbf{r}_a)}{\partial\mathbf{r}_a}, \text{ and } \nabla m = \frac{\partial m(\mathbf{r}_s)}{\partial\mathbf{r}_s}. \tag{3.51}$$

where $\mathbf{r}_s$ and $\mathbf{r}_a$ are position vectors which belong to two distinct coordinate systems for the Ising-type system ($\mathbf{r}_s$) and asymmetric system ($\mathbf{r}_a$). When Eq. 3.47 is solved for m, and the resulting expression is substituted into Eq. 3.48, one finds

$$\frac{\partial\hat{\rho}(\mathbf{r}_a)}{\partial\mathbf{r}_a} \simeq \left[1 + (a_\lambda - a)m - b\left(\frac{\partial\hat{s}}{\partial m}\right)_t\right]\frac{\partial\hat{\rho}(\mathbf{r}_a)}{\partial\mathbf{r}_s}. \tag{3.52}$$

The density can be eliminated from both sides of this equation by dividing through by $\partial\hat{\rho}(\mathbf{r}_a)/\partial\mathbf{r}_s$. The resulting differential relation can be integrated to produce the full coordinate transformation

$$\mathbf{r}_s \simeq \mathbf{r}_a + (a_\lambda - a)\int m d\mathbf{r}_a - b\int\left(\frac{\partial\hat{s}}{\partial m}\right)_t d\mathbf{r}_a. \tag{3.53}$$

As seen from Eq. 1.40, $\Delta s = t/g - (1/2)m^2$ for the mean-field EOS, so that the mean-field coordinate transformation reduces to

$$\hat{\mathbf{r}}_s \simeq \hat{\mathbf{r}}_a + (a_\lambda + b - a)\int m\mathrm{d}\hat{\mathbf{r}}_a. \tag{3.54}$$

The mean-field coordinate transformation is determined solely by integrating the magnetization.

The derivation of the complete scaling EOS is easily extended to include the new gradient terms. The transformations for the critical portion of the Helmholtz

energy $\Delta\tilde{f}$, which was defined in Eq. 1.25, and its natural variables are found to be

$$\Delta T = t - bh, \tag{3.55}$$

$$\Delta\rho = m + am^2 + b\Delta s - ct, \tag{3.56}$$

$$\nabla\hat{\rho} = [1 + (a + a_\lambda)m]\,\nabla m, \tag{3.57}$$

$$\Delta\tilde{f} = (1 + am)\Psi + b(\Delta s)h + \frac{1}{2}a_\lambda m|\nabla m|^2. \tag{3.58}$$

The gradient dependence of the symmetric Helmholtz energy given by Eq. 3.31 is $\Psi = \Psi_0 + (1/2)|\nabla m|^2$. Therefore, when the Helmholtz energy is separated into gradient dependent and independent portions, it takes on the expected form

$$\Delta\tilde{f} = \Delta\tilde{f}_0 + \frac{1}{2}\hat{\mathbf{w}} \cdot \nabla\rho. \tag{3.59}$$

This result justisfies our use of the simplified complete scaling transformations (Eqs. 3.41-3.44), and our assertion that these transformations capture all leading sources of asymmetry.

3.3.1 Equilibrium conditions

In this section we will derive an equilibrium condition, in the form of a differential equation, which can be used determine the spatial variations of the density in a system with coexisting, bulk liquid and vapor phases that are separated by an interfacial region. As in the previous sections, we assume that all thermodynamic quantities are smooth functions of the spatial coordinates. For an inhomogeneous system, thermodynamic equilibrium is specified by

$$\frac{\delta}{\delta\hat{\rho}}\left(\Delta\tilde{f} - \hat{\mu}_{\rm exc}\Delta\rho\right) = 0, \tag{3.60}$$

where $\hat{\mu}_{\rm cxc}$ is the chemical potential found at coexistence in the bulk phases ($\nabla\rho = 0$), which depends only on T. Our $\hat{\mu}_{\rm cxc}$ is equivalent to the standard definition of a chemical potential, which is uniform throughout an equilibrium system. The first integral of this equation is

$$\hat{f}_0 - \hat{\mu}_{\rm cxc}\hat{\rho} = \frac{1}{2}\hat{\mathbf{w}} \cdot \nabla\hat{\rho}, \tag{3.61}$$

where we maintain the convention that a subscript 0 denotes the gradient-free portion of a function. The derivative in Eq. 3.60 removes spatially uniform contributions to this equation such as pure functions of ΔT. To linear order in the asymmetry, the chemical potential at coexistence, as seen from Eqs. 3.41-3.44 is $\Delta\mu_{\rm cxc} = -a\Phi_{\rm cxc}$. In terms of symmetric variables, the left and right hand sides of Eq. 3.61 are

$$\hat{f}_0 - \hat{\mu}_{\rm cxc}\hat{\rho} = (1 + am)\left[\Psi_0 - \Psi_{\rm cxc}\right] + \Psi_{\rm cxc} + b(\Delta s)h_0, \tag{3.62}$$

and

$$\frac{1}{2}\hat{\mathbf{w}} \cdot \nabla\hat{\rho} = \frac{1}{2}\left[1 + (a + a_\lambda)m\right]|\nabla m|^2. \tag{3.63}$$

In the symmetric limit, $a = b = a_\lambda = 0$, Eq. 3.61 reduces to

$$\Psi_0 - \Psi_{\rm cxc} = \frac{1}{2}|\nabla m|^2. \tag{3.64}$$

The solution of this equation is given by the symmetric interfacial profile. In the mean-field limit, this is given by Eq. 3.3, and at $O(\epsilon)$ by Eq. 3.8. The asymmetric interfacial profile cannot be found by applying the complete scaling transformations to the symmetric interfacial profile. The result would not satisfy Eq. 3.61. An

equilibrium profile in the symmetric system does not transform into an equilibrium profile in the asymmetric system and vice versa. Equation 3.61 must be solved independently, and then the complete scaling transformations can be applied.

The extra Ψ_{cxc} in Eq. 3.64 is purely a function of t. However, the "symmetric" temperature t carries spatial dependence via μ. Therefore Ψ_{cxc} cannot be omitted from Eq. 3.64. The spatial dependence of t is isolated by expanding Ψ in the asymmetry coefficient b as,

$$\Psi(t) \simeq \Psi|_{t=\Delta T} - b(\Delta s)h. \tag{3.65}$$

This leads to a mixed representation that uses T, m, and ∇m as primary variables. This conceptually awkward choice is justified by the simplicity of the resulting equilibrium condition, specifically, Eq. 3.61 becomes,

$$(1 - a_\lambda m)\left[\Psi_0(m,t) - \Psi_{\text{cxc}}(t)\right]\big|_{t=\Delta T} = \frac{1}{2}|\nabla m|^2. \tag{3.66}$$

This differential equation can be solved to determine the magnetization profile.

The complete scaling density depends on both the magnetization and the entropy. The magnetization profile is found by solving Eq. 3.66 perturbatively. Since the entropy enters the profile as an asymmetric correction, only the symmetric entropy profile is needed, but this still must be calculated directly from the Ising-type EOS. First, we will treat the case $b = 0$, *i.e.*, no entropy term, in Sec. 3.4 and then we will derive and incorporate the entropy profile in Sec. 3.5.

3.4 Asymmetric profile ($b = 0$)

In this section, we will derive the magnetization profile, at $O(\epsilon)$, that solves Eq. 3.66. This can be done perturbatively by searching for a solution of the form $m(z_s) = m^{(0)}(z_s) + a_\lambda m^{(1)}(z_s)$, where $m^{(0)}$ is given by Eq. 3.8. We will again take the variation of the profile to be along the z-direction. The Helmholtz energy is expanded around the symmetric solution as

$$\Psi = \Psi|_{m=m^{(0)}} + a_\lambda m^{(1)} \left.\frac{\partial \Psi}{\partial m}\right|_{m=m^{(0)}}. \tag{3.67}$$

The zeroth and first order equations are found to be,

$$\frac{1}{2}\left(\frac{\partial m^{(0)}}{\partial z_s}\right)^2 = \Delta\Psi|_0\,, \tag{3.68}$$

and

$$\frac{\partial m^{(1)}}{\partial z_s} = \left(\frac{\partial m^{(0)}}{\partial z_s}\right)^{-1} \left.\frac{\partial \Delta\Psi}{\partial m}\right|_0 m^{(1)} + \frac{1}{2} m^{(0)} \left(\frac{\partial m^{(0)}}{\partial z_s}\right), \tag{3.69}$$

where $\Delta\Psi|_0 = [\Psi_0 - \Psi_{\text{cxc}}]|_{t=\Delta T, m=m^{(0)}}$. The zeroth order equation reproduces Eq. 3.8. The first order equation for $m^{(1)}$ can be cast in the form

$$\frac{\partial m^{(1)}}{\partial z_s} = -p \cdot m^{(1)} + q, \tag{3.70}$$

where

$$p = \left(\frac{\partial m^{(0)}}{\partial z_s}\right)^{-1} \left.\frac{\partial \Delta\Psi}{\partial m}\right|_0 = -\frac{\partial}{\partial z_s} \log\left(\frac{\partial m^{(0)}}{\partial z_s}\right), \tag{3.71}$$

and

$$q = \frac{1}{2} m^{(0)} \left(\frac{\partial m^{(0)}}{\partial z_s}\right), \tag{3.72}$$

and where the zeroth order equation, rewritten as $\partial_z^2 m^{(0)} = \partial\Delta\Psi/\partial m|_0$, has been used to express the second equality for p. This differential equation has the general

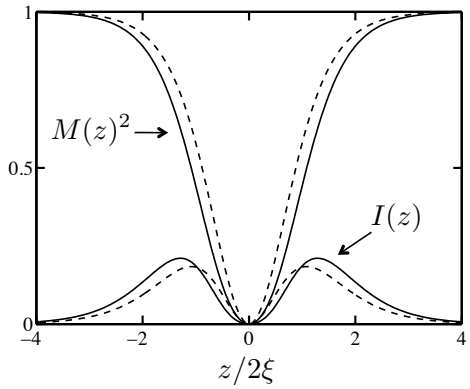

Figure 3.2: The interfacial profile function $I(z)$ and the bulk contribution $M(z)^2$ given by Eqs. 3.75 and 3.9. The corresponding mean-field functions are shown as dashed curves.

solution

$$m^{(1)}(z_s) = \frac{\int_0^{z_s} dz' \, \exp\left[\int_0^{z'} dz'' \, p(z'')\right] q(z')}{\exp\left[\int_0^{z_s} dz' \, p(z')\right]}, \tag{3.73}$$

from which it follows that,

$$m^{(1)}(z_s) = -\frac{1}{2}\partial_{z_s} m^{(0)}(z_s) \int_0^{z_s} m^{(0)}(z')dz'. \tag{3.74}$$

This type of functional dependence reappears frequently, so we define

$$I(z) = \partial_z M(z) \int_0^z M(z')dz', \tag{3.75}$$

with $M(z)$ given by Eq. 3.9. The full solution of Eq. 3.66 is,

$$m(z_s) \simeq m^{(0)}(z_s) - \frac{1}{2} a_\lambda (m_0)^2 I(z_s), \tag{3.76}$$

where $m_0 = B_0|\Delta T|^\beta$ is the amplitude of the magnetization. The function I is plotted in Fig. 3.2 for M given by Eq. 3.9. It only contributes to the interfacial region and does not affect the bulk properties.

For $b = 0$, the transformation, Eq. 3.53, between the asymmetric coordinate

and the symmetric coordinate is

$$z_s \simeq z_a + (a_\lambda - a)\int_0^{z_a} m^{(0)}(z')dz'. \tag{3.77}$$

The zeroth order solution can therefore be expanded in the asymmetry as

$$\begin{aligned} m^{(0)}(z_s) &\simeq m^{(0)}(z_a) + \partial_{z_a} m^{(0)}(z_a)\left\{(a_\lambda - a)\int_0^{z_a} m^{(0)}(z')dz'\right\} \\ &\simeq m^{(0)}(z_a) + (a_\lambda - a)(m_0)^2 I(z_a) \end{aligned} \tag{3.78}$$

The full magnetization profile, expressed in terms of the asymmetric coordinate is found by combining Eqs. 3.76 and 3.78 to yield,

$$m(z_s) \simeq m^{(0)}(z_a) + \left(\frac{a_\lambda}{2} - a\right)(m_0)^2 I(z_a). \tag{3.79}$$

When this profile is combined with Eq. 3.47, the density profile, for $b = 0$, is found to be

$$\begin{aligned} \Delta\rho(z_a) &\simeq B_0|\Delta T|^\beta M(z_a) + c|\Delta T| \\ &+ (B_0)^2|\Delta T|^{2\beta}\left[aM(z_a)^2 + \left(\frac{a_\lambda}{2} - a\right)I(z_a)\right]. \end{aligned} \tag{3.80}$$

The profile function M^2, which contributes to the bulk properties and disappears at the interface, is also plotted in Fig. 3.2 along with its mean-field counterpart.

The entropy follows the magnetization for the mean-field EOS, so that

$$\Delta\rho = m(z_s) + \left(a - \frac{1}{2}b\right)m(z_s)^2 + \left(c - \frac{b}{g}\right)|\Delta T|. \tag{3.81}$$

The full mean-field profile, $b \neq 0$, can therefore be found using the $b = 0$ result found in this section. The mean-field zeroth order profile is given by Eq. 3.3, and the coordinate transformation Eq. 3.54 becomes,

$$z_s \simeq z_a + (a_\lambda + b - a)\left\{\ln\left[\cosh\left(\frac{z_a}{2\xi}\right)\right] + k_0\right\}2\xi, \tag{3.82}$$

where k_0 is the constant of integration. In mean-field,

$$I(z) = \frac{\ln[\cosh(z/2\xi)]}{\cosh^2(z/2\xi)}, \tag{3.83}$$

which is also plotted in Fig. 3.2. The full mean-field excess density is,

$$\begin{aligned} \overline{\Delta\rho} &= (\Delta\rho_0)^2 \left[\left(a - \frac{1}{2}b \right) \tanh^2(\hat{z}_a) + \left(\frac{1}{2}a_\lambda + b - a \right) \frac{\ln[\cosh(\hat{z}_a)] + k_0}{\cosh^2(\hat{z}_a)} \right] \\ &+ (c - b/g)|\Delta T|, \end{aligned} \tag{3.84}$$

where $\hat{z}_a = z_a/2\xi$. This can also be written in terms of the mean-field Landau coefficients as,

$$\begin{aligned} \Delta\rho &= (\Delta\rho_0)^2 \left\{ \left(\frac{u_5}{20} - \frac{u_\lambda}{3} \right) \tanh^2(\hat{z}_a) + \left(\frac{u_5}{10} - \frac{u_\lambda}{3} \right) \frac{\ln[\cosh(\hat{z}_a)] + k_0}{\cosh^2(\hat{z}_a)} \right. \\ &+ \left. \left(\frac{u_3}{6} - \frac{3}{20}u_5 + \frac{u_\lambda}{3} \right) \right\}. \end{aligned} \tag{3.85}$$

The Fisher and Wortis result is reproduced in the limit $u_\lambda = 0$ if the integration constant is selected as $k_0 = 3/2$. The asymmetric gradient modifies the amplitude of each term in the excess density, but does not create any new types of spatial dependence.

Equation 3.14, which was derived in the approximation $u_\lambda = 0$, cannot be used to calculate the Tolman's length from the full mean-field profile presented in Eq. 3.85. Barrett [78, 79] has derived a generalization of Eq. 3.14 that includes the effects of u_λ. Barrett's expression for Tolman's length can be written as

$$\delta_{\mathrm{T}} = \frac{\int_{-\infty}^{\infty} dz\ z(1 + \frac{2}{3}u_\lambda\Delta\rho)(\partial_z\rho)^2}{\int_{-\infty}^{\infty} dz\ (1 + \frac{2}{3}u_\lambda\Delta\rho)(\partial_z\rho)^2} - \frac{\int_{-\infty}^{\infty} dz\ z\partial_z\rho}{\int_{-\infty}^{\infty} dz\ \partial_z\rho}. \tag{3.86}$$

For the special case $u_\lambda = 0$ this reproduces Eq. 3.14. When Eq. 3.85 is combined with Eq. 3.86, the resulting Tolman's length is found to be

$$\delta_{\mathrm{T}} = \frac{1}{12} \left(u_5 + \frac{2}{3}u_\lambda \right) \Delta\rho_0\xi. \tag{3.87}$$

All bulk terms make zero contribution to Tolman's length. Only the interfacial term I contributes. This reflects the fact that Tolman's length is proportional to the interfacial adsorption [64]. The asymmetric gradient modifies the amplitude of Tolman's length. This result implies that Tolman's length cannot be derived from exclusively bulk thermodynamic considerations. Both u_5 and u_λ are expected to be negative, so the mean-field Tolman's length of a droplet is still expected to be negative for $u_\lambda \neq 0$.

3.5 Interfacial entropy profile

As follows from Eqs. 1.40 and 3.3, the mean-field entropy profile is simply related to the magnetization profile,

$$\Delta s(z) = \frac{t}{g} - \frac{1}{2}m(z)^2 = \frac{t}{g} - \frac{1}{2}(m_0)^2 \tanh^2\left(z/2\xi\right). \tag{3.88}$$

The entropy density takes on its maximum value at $z = 0$, where the bulk phases coexist in equal proportion. When fluctuations are included, this picture becomes more complicated. In this section, we calculate the entropy profile to $O(\epsilon)$ following Ohta and Kawasaki's work on the magnetization profile [58].

As shown in Appendix A, the Ising Helmholtz energy, in the one-loop approximation, is given by

$$\Psi = \mathcal{H}|_{\phi=m} + \frac{1}{2}\mathrm{Tr}\left\{\ln \mathcal{H}^{(2)}\right\}, \tag{3.89}$$

where $\mathcal{H}$ is the renormalized Ising Hamiltonian and the fluctuation operator $\mathcal{H}^{(2)}$ is

$$\mathcal{H}^{(2)} = \left[-\nabla^2 + t + \frac{g}{2}m^2\right]\delta(x_1 - x_2). \tag{3.90}$$

The entropy density is therefore

$$\Delta s = -\left.\frac{\partial \mathcal{H}}{\partial t}\right|_{\phi=m} - \frac{1}{2}\mathrm{Tr}\left\{\left(\mathcal{H}^{(2)}\right)^{-1}\right\}. \tag{3.91}$$

For a uniform system, the magnetization in $\mathcal{H}^{(2)}$ does not vary in space, and the trace is easily performed. For a system with an interface, m may be taken to be the mean-field profile in Eq. 3.3, and the eigenfunctions and eigenvalues of $\mathcal{H}^{(2)}$ are significantly more complicated. Fortunately, the trace has already been performed by Ohta and Kawasaki in Ref. [58] in the context of calculating the magnetization profile, with the result,

$$\begin{aligned}\frac{g}{2}\mathrm{Tr}\left\{\left(\mathcal{H}^{(2)}\right)^{-1}\right\} &= (2|t|)^{-\epsilon/2}\left[\frac{1}{2}\left(1+\frac{\epsilon}{2}\right)\mathrm{sech}^2(\hat{z}) - \frac{1}{3}\right] \\ &- \frac{\epsilon\pi}{2\sqrt{3}}\mathrm{sech}^2(\hat{z})\tanh^2(\hat{z}),\end{aligned} \tag{3.92}$$

where $\hat{z} = z/2\xi$. The total expression for Δs, when expanded to first order in ϵ, is

$$\begin{aligned}\Delta s = \frac{t}{g} - \frac{1}{2}m^2 &- \frac{\epsilon}{6}\left(\frac{t}{g}+\frac{1}{2}m^2\right)\left[1+\ln\left(2|t|\right)\right] \\ &- \frac{\epsilon}{6}\left\{3-(3+\sqrt{3}\pi)\frac{gm^2}{6|t|}+\sqrt{3}\pi\left(\frac{gm^2}{6|t|}\right)^2\right\}\frac{|t|}{g},\end{aligned} \tag{3.93}$$

where the mean-field magnetization profile has been used to eliminate the hyperbolic functions at $O(\epsilon)$. The term in the braces is zero for $m = (6|t|/g)^{1/2}$. Using the definitions of the amplitudes and exponents found in Appendix A, we can write this as

$$\Delta s(z) = \frac{A_0^-}{1-\alpha}t|t|^{-\alpha} + \left(A_0^- - A_0^+/2^\alpha\right)t|t|^{-\alpha}S\left(z\right), \tag{3.94}$$

where

$$S(z)+1 = M(z)^2\left[1-\frac{\epsilon\pi}{6\sqrt{3}}\mathrm{sech}^2(\hat{z})\right], \tag{3.95}$$

and M is given by Eq. 3.9. The function $S(z)$ is negative and vanishes in the bulk phases at $z = \pm\infty$. At the center of the interface, one has

$$\Delta s(z=0) = \frac{A_0^+/2^\alpha}{1-\alpha}\left(1+\frac{\epsilon}{2}\right)t|t|^{-\alpha}. \tag{3.96}$$

Interestingly, this does not quite match the entropy above, even though the magnetization is zero at $z = 0$, because $\nabla m \neq 0$ at $z = 0$. As a practical matter, it would be desirable to have an entropy profile that "follows" the magnetization profile, as in the mean-field case. To this end, we will replace Eq. 3.95 by the approximation

$$S(z) + 1 \simeq M(z)^2. \tag{3.97}$$

This approximation does not alter the underlying physical picture, but will affect some numerical factors, which, at the one-loop level were not precise to begin with. It will great simplify the remaining calculations and applications.

The coordinate transformation, Eq. 3.53, depends on the derivative of the entropy with respect to the magnetization, which is calculated from Eq. 3.93 as,

$$\begin{aligned}\left(\frac{\partial s}{\partial m}\right)_t &= 2\left(\frac{A_0^- - A_0^+/2^\alpha}{B_0}\right)|t|^{1-\alpha-\beta}M\left\{1-\frac{\epsilon\pi}{6\sqrt{3}}\left[1-2\tanh^2\right]\right\} \\ &\simeq 2\left(\frac{A_0^- - A_0^+/2^\alpha}{B_0}\right)|t|^{1-\alpha-\beta}M,\end{aligned} \tag{3.98}$$

where in the second equality, we have employed Eq. 3.97. This expression will be used in the following section.

3.5.1 Full interfacial density profile

The full density profile is found by combining the magnetization profile, Eq. 3.79, the entropy profile, Eq. 3.94 , and the coordinate transformation, Eq. 3.53.

The result can be divided into two parts. One part, $\Delta\rho_{\rm B}$, only contributes to the bulk properties found at $z \to \pm\infty$, the other, $\Delta\rho_{\rm I}$, only contributes to the interfacial region. For these we find

$$\Delta\rho(z) = \Delta\rho_{\rm B} + \Delta\rho_{\rm I}, \tag{3.99}$$

with,

$$\begin{aligned} \Delta\rho_B(z) &= B_0|\Delta T|^{\beta}M(z) + a\left(B_0\right)^2|\Delta T|^{2\beta}M(z)^2 \\ &- b\frac{A_0^-}{1-\alpha}|\Delta T|^{1-\alpha} + c|\Delta T|, \end{aligned} \tag{3.100}$$

and

$$\begin{aligned} \Delta\rho_I(z) &= \left(\frac{1}{2}e - a\right)\left(B_0\right)^2|\Delta T|^{2\beta}I(z) \\ &+ b\left(A_0^- - \frac{A_0^+}{2^{\alpha}}\right)|\Delta T|^{1-\alpha}[2I(z) + S(z)]. \end{aligned} \tag{3.101}$$

The bulk portion is similar to what one would expect from a naive interpretation of the complete scaling density.

As was the case for Eq. 3.8, the interfacial profile in Eq. 3.99 is derived in the first order ϵ-expansion. As discussed previously, this approach ignores capillary-wave like fluctuations which destroy the interface in the absence of gravity. The results derived in this section could be modified to account for issues like gravity by using a different expression for the symmetric magnetization profile. The extended complete scaling transformations are intended as a method for generating an asymmetric profile from a symmetric profile and the exact nature of the profile does not matter.

3.5.2 Interfacial heat capacity

The entropy profile in Eq. 3.94 shows that the entropy deviates from its bulk value in the interfacial region. This implies that the heat capacity also deviates from its bulk value. The total heat capacity can be interpreted as consisting of two parts, the bulk heat capacity and the interfacial heat capacity. In this section we use the entropy profile, Eq. 3.94, to analyze interfacial heat capacity. We consider a system, below its critical point, confined to a cylindrical geometry of cross-sectional area Σ, and length L, oriented so that interface lies in the x-y plane, perpendicular to axis of the cylinder

The interfacial entropy density Δs_Σ can be approximated, assuming $L \gg \xi$, as

$$\Delta s_\Sigma = \frac{1}{L}\int_{-\infty}^{\infty} \left[\Delta s(z) - \Delta s(z=\infty)\right] dz = -k\left(\frac{\xi}{L}\right)\frac{A_0^-}{1-\alpha} t|t|^{-\alpha}, \tag{3.102}$$

with

$$k = 3\left(1 + \frac{\epsilon}{6}\left[\frac{\pi}{\sqrt{3}} - \frac{\ln 2}{3} - 1\right]\right). \tag{3.103}$$

The interfacial entropy is positive and results from the "mixing" of the two coexisting phases. The interfacial heat capacity is related to the interfacial entropy by $C_\Sigma/\hat{T} = (\partial s_\Sigma/\partial t)$, and is therefore,

$$\frac{C_\Sigma}{\hat{T}} = -k\left(1 - \frac{\nu}{1-\alpha}\right)\left(\frac{\xi}{L}\right) A_0^- |t|^{-\alpha}. \tag{3.104}$$

The interfacial heat capacity diverges as $C_\Sigma \sim -|t|^{-(\alpha+\nu)}$. The value of the critical exponent is $\alpha+\nu \simeq 0.74$, which leads to a stronger divergence than the corresponding mean-field prediction $C_\Sigma \sim |t|^{-1/2}$. If we extrapolate to $d = 3$ by taking $\epsilon \to 1$, we

find $k \simeq 3.3$. The interfacial entropy makes two contributions to the interfacial heat capacity: the first is due to the variation of the interfacial width and the second is due to the variation of the bulk entropy. The net result is a reduction of the heat capacity relative to the bulk value. Similar behavior has been found for the surface heat capacity [80].

The form of the interfacial heat-capacity suggests that total heat capacity of the system takes the form,

$$\frac{C_\rho}{\hat{T}} \simeq \frac{C_L}{\hat{T}} \left[1 - k \left(1 - \frac{\nu}{1-\alpha} \right) \frac{\xi}{L} \right], \tag{3.105}$$

where C_L is the bulk heat-capacity of the system, which approaches the total heat capacity as $L \to \infty$. In this form, the divergence of the interfacial heat capacity can be understood as an additional finite-size effect, produced when the correlation length, *i.e.*, the interfacial width, approaches the system size L. In a finite system, the extent of the fluctuations are constrained by the size of the system, and C_L will also be modified by terms of order $\sim \xi/L$ [81], such that

$$C_L - C_{L=\infty} \sim -\frac{\xi}{L}. \tag{3.106}$$

The interfacial reduction of the heat capacity occurs only below T_c, where as the finite-size modifications of the heat capacity are present above and below the critical point. This difference might allow the interfacial heat capacity reduction to be observed in simulations or experiments in which other finite-size effects are present. However, the interfacial reduction will only be noticeable very close to T_c. Typically, for $t \simeq 10^{-4}$, $\xi \simeq 0.5$ μm. To make the effect detectable one should have $L \lesssim 10$ μm. More details on finite-size scaling can be found in the review by Barber [82].

3.6 Tolman's length

We are now in a position to investigate the behavior of Tolman's length near the critical point. The mean-field expression for Tolman's length found by Fisher and Wortis can be written in terms of the Landau expansion coefficients (Eq. 2.29) as

$$\delta_{\mathrm{T}} = \frac{1}{12}\frac{f_5}{f_4}\left(\frac{6f_2|\Delta T|}{f_4}\right)^{1/2}\left(\frac{1}{2f_2|\Delta T|}\right)^{1/2}. \tag{3.107}$$

When the temperature dependent coefficients from the $O(\epsilon)$ EOS in Sec. 2.2 are substituted into this equation it yields

$$\delta_{\mathrm{T}} = -\left[\frac{5}{4}a|\Delta T|^{\beta-\nu} - \frac{5}{3}b|\Delta T|^{1-\alpha-\beta-\nu}\right]B_0\xi_0^-. \tag{3.108}$$

This expression matches the prediction of Anisimov [69], Eq. 3.16, when we use the $O(\epsilon)$ relation $\beta/\Gamma_0^- \simeq 1$. A purely thermodynamic expression of this type should be valid in the limit $u_\lambda = 0$, when there are no contributions from the asymmetric gradient term.

To study Tolman's length for $u_\lambda \neq 0$, the asymmetric profile must be used. The Barret expression for δ_{T}, Eq. 3.86, was derived for a mean-field equation of state, however, it may still serve as a reasonable approximation at $O(\epsilon)$, for the same reason that the surface tension calculated at $O(\epsilon)$ with Eq. 3.6 is very close to the actual surface tension. When the full density profile, Eq. 3.99 is substituted into Eq. 3.86 for δ_{T}, one finds,

$$\begin{aligned}\frac{\delta_{\mathrm{T}}}{2\xi} = &\left[\frac{1}{3}u_\lambda(2k_3 - k_1 - k_2) - \frac{1}{2}a(3k_2 - k_1)\right]B_0|\Delta T|^{\beta} \\ &+b(4k_1 + 2k_2)\left(\frac{A_0^- - A_0^+/2^\alpha}{B_0}\right)|\Delta T|^{1-\alpha-\beta},\end{aligned} \tag{3.109}$$

where k_1, k_2, and k_3 are numerical coefficients given by the integrals,

$$k_1 = 2\frac{\int dx\, x\, M\,[\partial_x M]^2}{\int dx\ (\partial_x M)^2} - \frac{\int dx\, x\, M \partial_x M}{\int dx\, \partial_x M}, \tag{3.110}$$

$$k_2 = 2\frac{\int dx\, \left(x\, \partial_x M \partial_x^2 M \int dx\, M\right)}{\int dx\ (\partial_x M)^2} - \frac{\int dx\, \left(x\, \partial_x^2 M \int dx\, M\right)}{\int dx\, \partial_x M}, \tag{3.111}$$

$$k_3 = \frac{\int dx\, x\, M\,[\partial_x M]^2}{\int dx\ (\partial_x M)^2}, \tag{3.112}$$

and where $x = z/2\xi$ is the integration variable and the limits of integration extend from $-\infty$ to ∞. These integrals evaluate to

$$k_1 = \frac{1}{5}\left(\frac{\epsilon\pi}{6\sqrt{3}}\right), \tag{3.113}$$

$$k_2 = \frac{5}{12} + \frac{7}{75}\left(\frac{\epsilon\pi}{6\sqrt{3}}\right), \tag{3.114}$$

$$k_3 = \frac{1}{4} + \frac{4}{15}\left(\frac{\epsilon\pi}{6\sqrt{3}}\right). \tag{3.115}$$

In the limit $\epsilon \to 1$, we find $k_1 \simeq 0.061$, $k_2 \simeq 0.44$, and $k_3 \simeq 0.33$. Based on Anisimov's expression for Tolman's length found in Eq. 3.16, it seems likely that the term proportional to b also contains a factor of β/Γ_0^- which cannot be resolved at $O(\epsilon)$. Tolman's length can be written compactly as

$$\frac{\delta_{\mathrm{T}}}{2\xi} = \delta_0|\Delta T|^\beta + \delta_1|\Delta T|^{1-\alpha-\beta} \tag{3.116}$$

In terms of the expansion coefficients, these amplitudes are found to be

$$\delta_0 \simeq -(0.25u_5 - 0.89u_\lambda)B_0, \tag{3.117}$$

$$\delta_1 \simeq (0.80u_5 - 2.26u_\lambda)\frac{A_0^- - A_0^+/2^\alpha}{B_0}. \tag{3.118}$$

Both coefficients, u_5 and u_λ, are expected to be negative, and consequently, unlike the mean-field case, the signs of δ_0 and δ_1 appear to depend sensitively on their

	HD	Ne	N_2	C_2H_4	C_2H_6	SF_6	$C_2Cl_3F_3$	C_7H_{16}
δ_0	-0.031	-0.013	-0.023	-0.047	-0.050	-0.263	-0.362	-0.521

Table 3.1: Estimates of Tolman's length amplitude δ_0

relative values. In the mean-field theory, and the scaling predictions based on that theory, the sign of Tolman's length is strictly negative. If $u_\lambda = 0$, δ_0 would be positive for a negative u_5. However, for positive mixing parameter a, as discussed at the end of Sec. 2.5, we have $|u_5| \lesssim 3.33|u_\lambda|$. Here, we see that δ_0 will be negative for $|u_5| \lesssim 3.56|u_\lambda|$. This bound for δ_0 is more stringent than that provided by the positivity of a. We can estimate the values of the Tolman's length amplitudes using the values of u_5 and u_λ found from fits to experimental coexistence curves in Chapter 2. For all of these coexistence curves a was found to be positive. The combined results of Table 2.2 and Eq. 3.117 are presented in Table 3.1. The leading amplitude δ_0 is found to be negative. The sign of δ_1 follows the sign of the asymmetry parameter b, but its magnitude is more uncertain, since, as discussed below Eq. 3.109, there may be numerical factors that are not resolved by the current $O(\epsilon)$ calculations.

The amplitude δ_0 depends on two coefficients and therefore cannot be part of a universal amplitude ratio, unless one of the coefficients is zero. If $u_\lambda = 0$, then

$$-\frac{\delta_0 B_0}{D_{2\beta}\xi_0^-} \simeq 1.27 \tag{3.119}$$

is a universal quantity, where $D_{2\beta}$ is the amplitude of the 2β contribution to the diameter. However, experimental evidence from Chapter 2 seems to suggest that $u_\lambda \neq 0$.

3.7 Summary and Conclusions

In Sec. 3.3, the complete scaling transformations were extended to inhomogeneous systems by including gradient mixing within the approximation $\eta = 0$. The remainder of the chapter considered the consequences these extended complete scaling transformations. A simplified form of the transformations is presented in Eqs. 3.41-3.44. These transformations predict a connection, Eq. 3.48, between the density gradient and the magnetization gradient, that we argued can be interpreted as a coordinate transformation, Eq. 3.53, between an asymmetric physical system and a symmetric Ising-type system. The subsection 3.3.1 demonstrates the complex connection between the equilibrium conditions for a planar density profile and a planar magnetization profile. The equilibrium condition was solved in Sec. 3.4, for the special case $b = 0$, with the result presented in Eq. 3.80. Based on this profile is was shown that the mean-field Tolman's length is still predicted to be negative for $u_\lambda \neq 0$. The solution for the full density profile, Eq. 3.99, was completed in subsection 3.5.1, after the interfacial entropy profile, Eq. 3.94, was derived in Sec. 3.5. The implications of the entropy profile for the interfacial heat capacity were discussed in Sec. 3.5.2. Finally Tolman's length was calculated from the full interfacial profile in Sec. 3.6. The resulting expression, Eq. 3.109, shares the temperature dependence of previous thermodynamic derivations, but differs significantly in its predictions of the amplitudes. In particular, u_λ appears to break a proposed universal amplitude ratio.

Chapter 4

Summary and Discussion

In this dissertation we have discussed different aspects of asymmetric fluid criticality. In Chapter 1, we provided an introduction to the general concepts associated with fluid criticality, which were then illustrated in the mean-field approximation. The results of Chapters 2 and 3 have previously been summarized in Secs.2.6 and 3.7 respectively. Although many of the ancillary results have independent merit, we recapitulate only the chief findings here. In Chapter 2, the RG treatment of fluid asymmetry and a set of simplified complete scaling transformations were shown to yield identical thermodynamic results at first order in $\epsilon = 4 - d$. Once the complete scaling exponent "2β" has been identified in the excess density, one cannot separately identify a distinct "θ_5" correction term at this order.

In Chapter 3, complete scaling was extended to inhomogeneous systems. This result was used to calculate the near-critical Tolman's length. The temperature dependence of Tolman's length was shown to agree with previous estimates, however, the amplitude of the leading contribution was shown to depend on the coefficient of the asymmetric gradient, which has previously been ignored in some treatments. The sign of Tolman's length was found to be negative in real fluids in agreement with other theoretical treatments and recent simulation results. In the remainder of this section, we will discuss some outstanding issues in an informal manner.

One of the unifying themes of this dissertation has been the importance of the asymmetric gradient contribution, both to the "proof" of complete scaling, and for determining the amplitude of Tolman's length. However to the best of the author's knowledge, little is known about the nature of this term. The coefficient f_1 in front of the square gradient in Eq. 3.20 is related to the direct correlation function $c(r;\rho)$ at position r, by [68],

$$f_1(\rho) = \frac{1}{6} k_{\mathrm{B}} T \int r^2 c(r;\rho) d\mathbf{r}. \tag{4.1}$$

This expression has been used to estimate the amplitude of the correlation length ξ_0^+, as found in the expansion $f_1 \simeq (\xi_0^+)^2[1 + (2/3)u_\lambda \Delta\rho]$, from the interparticle potential $u(r)$ by

$$(\xi_0^+)^2 \sim -\frac{1}{6} \int r^2 u(r) d\mathbf{r}. \tag{4.2}$$

It appears the same has not been done for u_λ. In particular it would be interesting to determine if there are intermolecular potentials for which u_λ is negligibly small in the critical region. Since u_5 is expected to be negative, this would imply that $a < 0$ and $b < 0$, and that the excess density would consequently exhibit a "wiggle". More precisely the second derivative of the excess density with respect to temperature would change sign in the critical region. The fact that this type of "wiggle" is not seen in experimental or simulation [83] results, indicates that u_λ cannot in general be ignored. Simulation data for specific forms of the interaction potential could be combined with fits to complete scaling predictions to determine how the asymmetry coefficients vary with interaction range and shape of the potential. Precise simulation data of near-critical coexistence curves have already been made for model

potentials such as the hardcore square-well [84, 83, 85]. It would be worthwhile to refit the numerical coexistence-curve data presented in these works in light of the findings of this disertation.

There are still unresolved issues surrounding the "proof" of complete scaling presented in Chapter 3. Nicoll's proof of revised scaling does not depend on the ϵ-expansion and holds to all orders. In this sense, revised scaling can be thought of as an exact "eigenoperator" of the asymmetric Hamiltonian. To explicitly demonstrate this, revised scaling was shown to hold at order ϵ^2. In the same spirit, we have shown that complete scaling holds to order ϵ. The next logical step would be to extend the demonstration of complete scaling to order ϵ^2. Initial calculations suggest that, unlike the revised scaling case, this is not a straightforward task. If complete scaling cannot be shown to hold at all orders, then perhaps it corresponds to an approximate "eigenoperator". In order to truly understand the relevance of complete scaling, it is necessary to understand why the normal RG formalism does not arrive at the same predictions as complete scaling. In Sec. 2.4 it was shown that the ϵ-expansion of the asymmetric "RG" EOS has two different interpretations at first order in ϵ, one identifies the exponent θ_5, the other matches complete scaling by identifying a 2β term, but not a distinct θ_5 term. The same physical system cannot be described by both of these interpretations. It seems as though there ought to be a way to isolate the correct, or physically meaningful, interpretation. Extending the work in this dissertation to second order in ϵ seems like a reasonable next step in this direction.

Thus far, the complete scaling mixing parameters have been found from fits to experimental coexistence curve data, with some work on the Yang-Yang anomaly.

Fluid asymmetry also affects properties like the susceptibility, and, as discussed in Chapter 3, the correlation length. If these were independently measured, values for the mixing parameters, and therefore the coefficients in the effective Hamiltonian, could be determined more accurately and more consistency. Experiments to measure the susceptibilities in the "bulk" portions of the coexisting phases via light scattering have previously been suggested. By varying the scattering angle, the asymmetry in the correlation length could be similarly probed.

The complete scaling equation of state developed in the ϵ-expansion was useful for comparison with the RG EOS, but is not practical for other applications. As mentioned in Chapter 2, a version of the complete scaling EOS based on a parametric model would be useful. The details of the resulting EOS still need to be worked out. A crossover EOS that correctly interpolates between the critical and mean-field regimes, and incorporates complete scaling, could be another useful extension.

Throughout this work we have discussed liquid-vapor systems without much reference to fluid mixtures. These systems are connected through the isomorphism principle, and we have used this connection to justify our seemingly narrow focus. However, there is one regard in which liquid-vapor systems and fluid mixtures are not identical, and that is the ease with which experiments can be conducted and accurate results can be obtained. Data for fluid mixtures is more abundant, can exhibit high degrees of asymmetry, and can be collected with good accuracy [86, 29]. For these reasons, it would be interesting to apply the current formulation of complete scaling to fluid mixtures in order to find experimental values for the mixing parameters and asymmetric Hamiltonian coefficients. This would require a minor modification, the

inclusion of an independent linear term, to the previous complete scaling fits for fluid mixtures, and should be relatively easy to execute.

The concepts used to extend complete scaling to inhomogeneous fluids could be applied to other thermodynamic fields, in particular to the electric field. To study the thermodynamics of the dielectric constant, it is necessary to include the electric field in the EOS. The implications of revised scaling for the near-critical dielectric constant were investigated by Sengers *et al.* [87]. Recently, this work was extended to complete scaling [88]. However, the implications for the complete scaling equation of state and the effects of the mixing-parameter c were not considered. A reconsideration in light of these developments could yield additional information.

Appendix A

Ising-type equation of state in the one-loop approximation

The general results of this Appendix can be found in many other sources, such as the chapter by Brezin *et al.* [37]. Our current purpose is to explicitly show some of details that are often omitted.

In this Appendix we will follow the convention that $k_{\mathrm{B}} = 1$, where k_{B} is Boltzmann's constant. The Ising- Helmholtz energy Ψ is related to the canonical partition function Z by

$$\Psi(m,t) = -T \ln Z. \tag{A.1}$$

The partition function can be written as a path integral, in terms of the continuous field-variable, ϕ, as

$$Z = \int \mathcal{D}\phi \exp\left\{ - \int dx \mathcal{H}\left[\phi(x)\right] \right\}, \tag{A.2}$$

where $\mathcal{H}$ is the Hamiltonian density, or Hamiltonian for short. To determine the leading effects of fluctuations, the integral can be approximated by expanding around the equilibrium value the field, namely, $\langle \phi \rangle = m$. This is known as the loop expansion. If $\phi = m + \delta\phi$, then the Hamiltonian is expanded in $\delta\phi$ as

$$\mathcal{H}\left[\phi(x)\right] = \mathcal{H}|_{\phi=m} + \frac{1}{2} \iint dx_1 dx_2 \mathcal{H}^{(2)}(x_1, x_2) \delta\phi(x_1) \delta\phi(x_2) + \cdots, \tag{A.3}$$

where the linear term is zero because $\langle \phi \rangle$ minimizes $\mathcal{H}$. We will not consider the

higher order terms in this expansion. The quadratic term is defined by

$$\mathcal{H}^{(2)}(x_1, x_2) = \left. \frac{\delta^2 \mathcal{H}}{\delta\phi(x_1)\delta\phi(x_2)} \right|_{\phi=m}. \tag{A.4}$$

The partition function can now be separated into two factors,

$$Z = \exp\left\{ -\int \mathcal{H}|_{\phi=m} \right\} \int \mathcal{D}\delta\phi \exp\left\{ -\int \mathcal{H}^{(2)} (\delta\phi)^2 \right\}, \tag{A.5}$$

where the Gaussian integral is evaluated as

$$\int \mathcal{D}\delta\phi \exp\left\{ -\frac{1}{2} \int \mathcal{H}^{(2)} (\delta\phi)^2 \right\} = \sqrt{\frac{2\pi}{\mathrm{Det}\mathcal{H}^{(2)}}}. \tag{A.6}$$

Taking the logarithm, we find the Helmholtz energy density

$$\Psi = \mathcal{H}|_{\phi=m} + \frac{1}{2}\mathrm{Tr}\left\{ \ln \mathcal{H}^{(2)} \right\} \tag{A.7}$$

This is the general EOS in the one-loop approximation. To proceed further, an explicit expression for the Hamiltonian is required.

The Ising-type Landau-Ginzburg-Wilson (LGW) Hamiltonian is given by

$$\mathcal{H}\left[\phi(x)\right] = -\frac{(t_0)^2}{2g_0} + \frac{1}{2} t_0 \phi^2 + \frac{g_0}{4!}\phi^4 + \frac{1}{2}|\nabla\phi|^2. \tag{A.8}$$

The asymptotic Ising mean-field EOS, Eq. 1.37 , is recovered from the first term in Eq. A.7, if $t_0 = t$ and $g_0 = g$. The second term provides the leading fluctuation corrections. For this reason, $\mathcal{H}^{(2)}$ can be called the "fluctuation operator". The bare Hamiltonian in Eq. A.8 does not yield finite results. Consequently, the "bare" coefficients, t_0 and g_0, must be renormalized. The renormalization conditions can be expressed in terms of the n-point irreducible vertex functions, $\Gamma^{(n)}$, and the renormalized coefficients, t and g, as

$$\Gamma^{(2)}\left(p_1, p_2; t_0, g_0\right)\big|_{p_i=0} = t, \tag{A.9}$$

$$\Gamma^{(4)}\left(p_1, p_2, p_3, p_4; t_0, g_0\right)\big|_{p_i=0} = g, \tag{A.10}$$

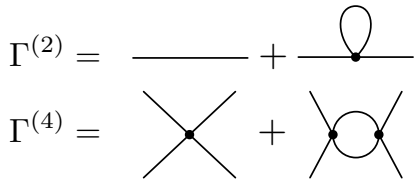

Figure A.1: Ising vertex-function diagrams up to one loop

where the vertex functions have been evaluated at zero momentum. The details of the renormalization scheme only affect non-universal terms, and are therefore unimportant. Renormalization at zero-momentum is a conceptually simple scheme, but it does not always yield the cleanest results. The vertex functions can be represented through diagrammatic expansions, in which each diagram corresponds to a particular integral with a numerical coefficient determined by standard counting rules. For the Ising-type Hamiltonian, the relevant diagrams are shown in Fig. A.1.

Reading off the terms from Fig. A.1, we find

$$t \simeq t_0 \left(1 - \frac{g_0}{2} J\right) + \delta t \tag{A.11}$$

$$g \simeq g_0 \left(1 - \frac{3}{2} g_0 J\right), \tag{A.12}$$

where the "mass shift" is

$$\delta t = -\frac{g_0}{2} \int_q \frac{1}{q^2}, \tag{A.13}$$

while one has

$$J = \int_0^\infty \frac{q^{d-1} dq}{(q^2+1)^2}. \tag{A.14}$$

The expressions for the bare coefficients, found by inverting Eqs. A.11 and

A.12 and linearizing in g, are

$$t_0 \simeq t\left(1+\frac{g}{2}J\right), \tag{A.15}$$

$$g_0 \simeq g\left(1+\frac{3}{2}gJ\right), \tag{A.16}$$

where the mass-shift, which does not affect our calculations, has been omitted. The first term in Eq. A.7 is now found to be

$$\mathcal{H}|_{\phi=m} = -\frac{t^2}{2g}+\frac{1}{2}tm^2+\frac{g}{4!}m^4+\frac{1}{4}\left(t^2+gtm^2+\frac{g^2}{4}m^4\right)J \tag{A.17}$$

If we denote the Ising mean-field EOS (Eq. 1.37) by $\bar{\Psi}$ to distinguish it from the fluctuation-modified Helmholtz energy Ψ, then the above equation can be compactly re-expressed as

$$\mathcal{H}|_{\phi=m} = \bar{\Psi}+\frac{(\bar{\Psi}'')^2}{4}J, \tag{A.18}$$

where $\bar{\Psi}'' = \partial^2\bar{\Psi}/\partial m^2$. In Nicoll's previous work [24], a different notation was used, namely, $\kappa^2 = \bar{\Psi}''$. For comparison with Nicoll's results, we will adopt this notation, so that

$$\kappa^2 = t+(g/2)m^2. \tag{A.19}$$

The mean-field theory correctly describes critical phenomena in $d > 4$ dimensions, where fluctuations do not affect the leading bulk exponents. Therefore, to investigate the critical phenomena in $d = 3$, we will follow Ref. [89] and make an expansion in ϵ, where $\epsilon = 4-d$, and then extrapolate to $\epsilon = 1$. This is known as "the ϵ-expansion". To leading order in ϵ, Eq. A.14 is found to be $J \approx 1/\epsilon - 1/2$. This value of J, correctly predicts all universal quantities at $O(\epsilon)$. However, it does not agree with the more commonly encountered value, found by applying slightly

more sophisticated renormalization conditions. In particular, a "mass-less" theory is typically renormalized at the symmetry point [37]. The choice of renormalization schemes only affects non-universal quantities, but in order to compare the current calculation with previous work, we will adopt the "standard" value from the mass-less renormalization scheme, specifically,

$$J \approx \frac{1}{\epsilon}\left(1+\frac{\epsilon}{2}\right). \tag{A.20}$$

This choice of J does not alter the previous discussion.

The fluctuation operator for the Ising-type Hamiltonian is,

$$\mathcal{H}^{(2)} = \left[-\nabla^2+\kappa^2\right]\delta(x_1-x_2), \tag{A.21}$$

Therefore the fluctuation correction is given by

$$\frac{1}{2}\mathrm{Tr}\ln\mathcal{H}^{(2)} = \frac{1}{2}\int_p \ln\left(p^2+\kappa^2\right) = \frac{1}{4\epsilon}\left(1-\frac{\epsilon}{4}\right)^{-1}\left(\kappa^2\right)^{2-\epsilon/2}, \tag{A.22}$$

where the integral has been performed in $d = 4-\epsilon$ dimensions. The two parts of the Helmholtz energy are combined to yield,

$$\Psi = \bar{\Psi} + \frac{\kappa^4}{4\epsilon}\left\{\epsilon J - \left(1-\frac{\epsilon}{4}\right)^{-1}\left(\kappa^2\right)^{-\epsilon/2}\right\}. \tag{A.23}$$

After expanding the terms in the braces to $O(\epsilon)$, we can compactly express the Ising-type EOS as

$$\Psi = \bar{\Psi} + \frac{g}{16}\left(\frac{\kappa^4}{g}\right)[2L+1], \tag{A.24}$$

where we have defined $L = \ln\kappa^2$. The second term, which comes from the fluctuation correction, is $O(\epsilon)$, although this is not explicitly manifest. To make the dependence

on ϵ explicit, one needs to substitute the fixed-point value of the coupling constant, $g^* = 2\epsilon/3$, into the coefficient of the second term so that $g^*/16 = \epsilon/24$.

Other thermodynamic properties of the system are easily derived from the Helmholtz energy. The magnetic field is found to be

$$h = tm + \frac{g}{6}m^3 + \frac{\epsilon}{6}m\kappa^2\left[L+1\right] \tag{A.25}$$

and the entropy density is

$$\Delta s = \frac{t}{g} - \frac{1}{2}m^2 - \frac{\epsilon}{6}\frac{\kappa^2}{g}\left[L+1\right]. \tag{A.26}$$

The magnetization at coexistence is found by solving $h = 0$, with the result, for $t < 0$,

$$m = \pm\left(\frac{6|t|}{g}\right)^{1/2}\left(1 - \frac{\epsilon}{6}\left[\ln 2|t| + 1\right]\right). \tag{A.27}$$

The ϵ-expansion is interpreted using the relation, $|t|^\epsilon \simeq 1 + \epsilon \ln|t|$. Therefore the magnetization can be written

$$m = \pm\frac{6}{g}\left(1 - \frac{\epsilon}{6}\left[\ln 2 + 1\right]\right)|t|^{1/2-\epsilon/6}. \tag{A.28}$$

The remaining amplitudes and exponents are found in a similar fashion. The value for the exponents and amplitudes are summarized in Tables A.1 and A.2. The amplitudes are not universal and depend on the particulars of the renormalization scheme. However, certain ratios of the amplitudes form universal quantities. For example, the susceptibility amplitude ratio is,

$$\frac{\Gamma_0^+}{\Gamma_0^-} = 2\left(1 + \frac{\epsilon}{2}\left[1 + \frac{\ln 2}{3}\right]\right) \simeq 2^{\gamma-1}\frac{\gamma}{\beta}. \tag{A.29}$$

Exponent:	β	α	γ	ν	η	δ
Value:	$\frac{1}{2}-\frac{\epsilon}{6}$	$\frac{\epsilon}{6}$	$1+\frac{\epsilon}{6}$	$\frac{1}{2}+\frac{\epsilon}{12}$	0	$3+\epsilon$
$\epsilon = 1$:	0.33	0.17	1.17	0.58	0	4

Table A.1: Critical exponents in the one-loop approximation at $O(\epsilon)$ based on the Ising-type EOS Eq. A.24

This matches the standard result at $O(\epsilon)$, whereas our value for the heat capacity amplitude ratio,

$$\frac{A_0^+}{A_0^-} = \frac{1}{4}\left(1+\frac{\epsilon}{6}\ln 2\right) \simeq \frac{2^\alpha}{4}, \tag{A.30}$$

only matches the standard result, $A_0^+/A_0^- = (2^\alpha/4)(1+\epsilon)$, to $O(1)$. While the one-loop expansion provides all other quantities to $O(\epsilon)$, a two-loop calculation is required to get the correct heat-capacity amplitude ratio at $O(\epsilon)$ [90].

Amplitude	Mean-field value
B_0	$\left(\frac{6}{g}\right)^{1/2}\left[1-\frac{\epsilon}{6}(\ln 2+1)\right]$
A_0^+	$\frac{1}{g}\left(1-\frac{\epsilon}{6}\right)$
A_0^-	$\frac{4}{g}\left[1-\frac{\epsilon}{6}(\ln 2+1)\right]$
Γ_0^+	$1-\frac{\epsilon}{6}$
Γ_0^-	$\frac{1}{2}[1-\frac{\epsilon}{6}(\ln 2+4)]$
ξ_0^+	$1-\frac{\epsilon}{12}$
ξ_0^-	$\frac{1}{\sqrt{2}}[1-\frac{\epsilon}{12}(\ln 2+4)]$

Table A.2: Critical amplitudes in the one-loop approximation at $O(\epsilon)$ based on the Ising-type EOS Eq. A.24

Bibliography

[1] P. M. Chaikin and T. C. Lubensky, *Principles of Condensed Matter Physics*. Cambridge University Press, 2000.

[2] M. E. Fisher, "The theory of equilibrium critical phenomena," Rep. Prog. Phys. **30**, 615 (1967).

[3] P. Heller, "Experimental investigations of critical phenomena," Rep. Prog. Phys. **30**, 731 (1967).

[4] L. P. Kadanoff, W. G otze, D. Hamblen, R. Hecht, E. A. S. Lewis, V. V. Palciauskas, M. Rayl, J. Swift, D. Aspnes, and J. Kane, "Static phenomena near critical points: Theory and experiment," Rev. Mod. Phys. **39**, 395 (1967).

[5] S. K. Ma, *Modern Theory of Critical Phenomena*. Westview Press, 1976.

[6] M. E. Fisher, "The renormalization group in the theory of critical behavior," Rev. Mod. Phys. **46**, 597 (1974).

[7] K. G. Wilson and J. Kogut, "The renormalization group and the ϵ expansion," Phys. Rep. **12**, 75 (1974).

[8] J. V. Sengers and J. M. H. Levelt Sengers, "Critical phenomena in classical fluids," in *Progress in Liquid Physics*, C. Croxton, Ed. Wiley, 1978, ch. 4.

[9] M. A. Anisimov, *Critical Phenomena in Liquids and Liquid Crystals*. Gordon and Breach, 1991.

[10] R. B. Griffiths and J. C. Wheeler, "Critical points in multicomponent systems," Phys. Rev. A **2**, 1047 (1970).

[11] M. A. Anisimov, A. Voronel, and E. E. Gorodetskii, "Isomorphism of critical phenomena," Sov. Phys. JETP **33**, 605 (1971).

[12] M. A. Anisimov, V. A. Rabinovich, and V. V. Sychev, *Thermodynamics of the Critical State of Individual Substances*. CRC press, 1995.

[13] M. E. Fisher, "Scaling, universality and renormalization group theory," in *Lecture Notes in Physics*, F. J. W. Hahne, Ed. Springer, 1983, vol. 186, p. 1.

[14] J. J. Rehr and N. D. Mermin, "Revised scaling equation of state at the liquid-vapor critical point," Phys. Rev. A **8**, 472 (1973).

[15] V. L. Pokrovskii, "Feasibility of experimental verification of the conformal invariance hypothesis," JETP Lett. **17**, 156 (1973).

[16] B. Widom and J. S. Rowlinson, "New model for the study of liquid-vapor phase transitions," J. Chem. Phys. **52**, 1670 (1970).

[17] N. D. Mermin, "Solvable model of a vapor-liquid transition with a singular coexistence-curve diameter," Phys. Rev. Lett **26**, 169 (1971).

[18] N. D. Mermin, "Lattice gas with short-range pair interactions and a singular coexistence-curve diameter," Phys. Rev. Lett **26**, 957 (1971).

[19] N. D. Mermin and J. J. Rehr, "Generality of the singular diameter of the liquid-vapor coexistence curve," Phys. Rev. Lett **26**, 1155 (1971).

[20] F. J. Wegner, "Critical exponents in isotropic spin systems," Phys. Rev. B **6**, 1891 (1972).

[21] C. Vause and J. Sak, "Non-Ising effects in the liquid-vapor transition: Equations of state," Phys. Rev. A **21**, 2099 (1980).

[22] M. LeyKoo and M. S. Green, "Consequences of the renormalization group for the thermodynamics of fluids near the critical point," Phys. Rev. A **23**, 2650 (1981).

[23] J. F. Nicoll and R. K. P. Zia, "Fluid-magnet universality: Renormalization-group analysis of ϕ^5 operators," Phys. Rev. B **23**, 6157 (1981).

[24] J. F. Nicoll, "Critical phenomena of fluids: Asymmetric Landau-Ginzburg model," Phys. Rev. A **24**, 2203 (1981).

[25] M. E. Fisher and G. Orkoulas, "The Yang-Yang anomaly in fluid criticality: Experiment and scaling theory," Phys. Rev. Lett. **85**, 696 (2000).

[26] Y. C. Kim, M. E. Fisher, and G. Orkoulas, "Asymmetric fluid criticality. I. Scaling with pressure mixing," Phys. Rev. E **67**, 061506 (2003).

[27] M. A. Anisimov and J. Wang, "Nature of asymmetry in fluid criticality," Phys. Rev. Lett. **97**, 025703 (2006).

[28] J. Wang and M. A. Anisimov, "Nature of vapor-liquid asymmetry in fluid criticality," Phys. Rev. E **75**, 051107 (2007).

[29] J. Wang, C. A. Cerdeiriña, M. A. Anisimov, and J. V. Sengers, "Principle of isomorphism and complete scaling for binary-fluid criticality," Phys. Rev. E **77**, 031127 (2008).

[30] J. Weiner, K. H. Langley, and N. C. Ford Jr., "Experimental evidence for a departure from the law of the rectilinear diameter," Phys. Rev. Lett. **32**, 879 (1974).

[31] M. W. Pestak, R. E. Goldstein, M. H. W. Chan, J. R. de Bruyn, D. A. Balzarini, and N. W. Ashcroft, "Three-body interactions, scaling variables, and singular diameters in the coexistence curves of fluids," Phys. Rev. B **36**, 599 (1987).

[32] A. Haupt and J. Straub, "Isochoric heat capacity measurements at the ciritcal isochore of SF_6 performed during the German spacelab mission D-2," Phys. Rev. E **59**, 1795 (1999).

[33] B. Widom, "Equation of state in the neighborhood of the critical point," J. Chem. Phys. **43**, 3898 (1965).

[34] R. B. Griffiths, "Thermodynamic functions for fluids and ferromagnets near the critical point," Phys. Rev. **158**, 176 (1967).

[35] A. Z. Patashinkiĭ and V. L. Pokrovskiĭ, "Behavior of ordered systems near transition point," Sov. Phys. JETP **23**, 292 (1966).

[36] T. D. Lee and C. N. Yang, "Statistical theory of equations of state and phase transitions. II. lattice gas and Ising model," Phys. Rev. **87**, 410 (1952).

[37] E. Brézin, J. C. Le Guillou, and J. Zinn-Justin, "Field theoretical approach to critical phenomena," in *Phase Transitions and Critical Phenomena*, C. Domb and M. S. Green, Eds. London: Academic Press, 1976, vol. 6, ch. 3.

[38] C. Domb, *The Critical Point*. Taylor & Francis, 1996.

[39] M. E. Fisher and S. Zinn, "The shape of the van der Waals loop and universal critical amplitude ratios," J. Phys. A: Math. Gen. **31**, L629 (1998).

[40] F. J. Wegner, "Corrections to scaling laws," Phys. Rev. B **5**, 4529 (1972).

[41] L. Cailletet and C. R. Mathias, "Recherches sur les densités des gaz liquéfiés et de leurs vapeurs saturées," C. R. Hebd. Seances Acad. Sci. **102**, 1202 (1886).

[42] L. Cailletet and C. R. Mathias, "Recherches sur la densité de l'acide sulfureux à l'état de liquide et de vapeur saturée," C. R. Hebd. Seances Acad. Sci. **104**, 1563 (1887).

[43] F. C. Zhang and R. K. P. Zia, "A correction-to-scaling critcal exponent for fluids at $O(\epsilon^3)$," J. Phys. A: Math. Gen. **15**, 3303 (1982).

[44] M. A. Anisimov, E. E. Gorodetskii, V. D. Kulikov, and J. V. Sengers, "Crossover between vapor-liquid and consolute critical phenomena," Phys. Rev. E **51**, 1199 (1995).

[45] C. N. Yang and C. P. Yang, "Critical point in liquid-gas transitions," Phys. Rev. Lett. **13**, 303 (1964).

[46] L. D. Landau and E. M. Lifshitz, *Statistical Physics*, 3rd ed. Elsevier Butterworth-Heineman, 1980.

[47] M. E. Fisher and B. U. Felderhof, "Phase transitions in one-dimensional cluster-interaction fluids IA. Thermodynamics," Ann. Phys. (N. Y.) **58**, 176 (1970).

[48] M. E. Fisher and B. U. Felderhof, "Phase transitions in one-dimensional cluster-interaction fluids IB. Critical behavior," Ann. Phys. (N. Y.) **58**, 217 (1970).

[49] P. Schofield, "Parametric representation of the equation of state near a critical point," Phys. Rev. Lett. **22**, 606 (1969).

[50] D. J. Wallace and R. K. P. Zia, "Parametric models and the Ising equation of state at order $O(\epsilon^3)$," J. Phys. C: Solid State Phys. **7**, 3480 (1974).

[51] M. A. Anisimov, V. A. Agayan, and P. J. Collings, "Nature of the blue-phase-III isotropic critical point: An analogy with the liquid-gas transition," Phys. Rev. E **57**, 582 (1998).

[52] E. T. Shimanskaya, I. V. Bezruchko, V. I. Basok, and Y. I. Shimanskiĭ, "Experimental determination of the critical exponent and of the asymmetric and non asymptotic corrections to the equation of the coexistence curve of freon-113," Sov. Phys. JETP **53**, 139 (1981).

[53] L. M. Artyukhovskaya, E. T. Shimanskaya, and Y. I. Shimanskiĭ, "The coexistence curve of heptane near the critical point," Sov. Phys. JETP **36**, 1140 (1973).

[54] V. A. Agayan, M. A. Anisimov, and J. V. Sengers, "Crossover parametric equation of state for Ising-like systems," Phys. Rev. E **64**, 026125 (2001).

[55] D. Jasnow, "Critical phenomena at interfaces," Rep. Prog. Phys. **47**, 1059 (1984).

[56] J. D. van der Waals, "Thermodynamische theorie der capillariteit in de onderstelling van continue dichtheidsverandering'," Verhandel. Konink. Akad. Weten. Amsterdam (Sect. 1) **1**, 56 (1893).

[57] J. S. Rowlinson, "Translation of J. D. van der Waals' 'the thermodynamik theory of capillarity under the hypothesis of a continuous variation of density'," J. Stat. Phys. **20**, 197 (1979).

[58] T. Ohta and K. Kawasaki, "Renormalization group approach to the interfacial order parameter profile near the critical point," Prog. Theor. Phys. **58**, 467 (1977).

[59] J. Rudnick and D. Jasnow, "ϵ expansion for the interfacial profile," Phys. Rev. B **17**, 1351 (1978).

[60] S. Fisk and B. Widom, "Structure and free energy of the interface between fluid phases in equilibrium near the critical point," J. Chem. Phys. **50**, 3219 (1969).

[61] J. S. Rowlinson and B. Widom, *Molecular Theory of Capillarity.* Clarendon Press, 1982.

[62] D. Jasnow and J. Rudnick, "Interfacial profile in three dimensions," Phys. Rev. Lett. **41**, 698 (1978).

[63] D. Jasnow, T. Ohta, and J. Rudnick, "Interfacial profile near tricritical points," Phys. Rev. B **20**, 2774 (1979).

[64] R. C. Tolman, "The effect of droplet size on surface tension," J. Chem. Phys. **17**, 333 (1949).

[65] M. P. A. Fisher and M. Wortis, "Curvature corrections to the surface tension of fluid drops: Landau theory and a scaling hypothesis," Phys. Rev. B **29**, 6252 (1984).

[66] A. E. van Giessen, E. M. Blokhuis, and D. J. Bukman, "Mean field curvature corrections to the surface tension," J. Chem. Phys. **108**, 1148 (1998).

[67] E. M. Blokhuis and J. Kuipers, "Thermodynamic expressions for the Tolman length," J. Chem. Phys. **124**, 074701 (2006).

[68] J. S. Rowlinson, "The critical exponent of Tolman's length," J. Phys. A: Math. Gen. **17**, L357 (1984).

[69] M. A. Anisimov, "Divergence of Tolman's length for a droplet near the critical point," Phys. Rev. Lett. **98**, 035702 (2007).

[70] A. E. van Giessen and E. M. Blokhuis, "Determination of curvature corrections to the surface tension of a liquid-vapor interface through molecular dynamics simulations," J. Chem. Phys. **116**, 302 (2002).

[71] M. J. Haye and C. Bruin, "Molecular dynamics study of the curvature correction to the surface tension," J. Chem. Phys. **100**, 556 (1994).

[72] P. R. ten Wolde and D. Frenkel, "Computer simulation study of gas-liquid nucleation in a Lennard-Jones system," J. Chem. Phys. **109**, 9901 (1998).

[73] A. E. van Giessen and E. M. Blokhuis, "Direct determination of the Tolman length from the bulk pressures of liquid drops via molecular dynamics simulations," J. Chem. Phys. **131**, 164705 (2009).

[74] M. Schrader, P. Virnau, and K. Binder, "Simulation of vapor-liquid coexistence in finites volumes: A method to compute the surface free energy of droplets," Phys. Rev. E **79**, 061104 (2009).

[75] B. J. Block, S. K. Das, M. Oettel, P. Virnau, and K. Binder, "Curvature dependence of surface free energy of liquid drops and bubbles: A simulation study," J. Chem. Phys. **133**, 154702 (2010).

[76] E. W. Hart, "Thermodynamics of inhomogeneous systems," Phys. Rev. **113**, 412 (1959).

[77] J. W. Cahn, "Free energy of a nonuniform system. II. Thermodynamic basis," J. Chem. Phys. **30**, 1121 (1959).

[78] J. Barrett, "First-order correction to classical nucleation theory: A density functional approach," J. Chem. Phys. **111**, 5938 (1999).

[79] J. C. Barrett, "Some estimates of the surface tension of curved surfaces using density functional theory," J. Chem. Phys. **124**, 144705 (2006).

[80] K. Binder, "Critical behaviour at surfaces," in *Phase Transitions and Critical Phenomena*, C. Domb and J. L. Lebowitz, Eds. London: Academic Press, 1983, vol. 8, ch. 3.

[81] M. E. Fisher and M. N. Barber, "Scaling theory for finite-size effects in the critical region," Phys. Rev. Lett. **28**, 1516 (1972).

[82] M. N. Barber, "Finite-size scaling," in *Phase Transitions and Critical Phenomena*, C. Domb and J. L. Lebowitz, Eds. London: Academic Press, 1983, vol. 8, ch. 2.

[83] Y. C. Kim and M. E. Fisher, "Singular coexistence-curve diameters: Experiments and simulations," Chem. Phys. Lett. **414**, 185 (2005).

[84] Y. C. Kim, M. E. Fisher, and E. Luijten, "Precise simulation of near-critical fluid coexistence," Phys. Rev. Lett. **91**, 065701 (2003).

[85] Y. C. Kim, "Yang-Yang anomalies and coexistence diameters: Simulation of asymmetric fluids," Phys. Rev. E **71**, 051501 (2005).

[86] C. A. Cerdeiriña, M. A. Anisimov, and J. V. Sengers, "The nature of singular coexistence-curve diameters of liquid-liquid phase equilibria," Chem. Phys. Lett. **424**, 414 (2006).

[87] J. V. Sengers, D. Bedeaux, P. Mazur, and S. C. Greer, "Behavior of the dielectric constant of fluids near a critical point," Physica A **104**, 573 (1980).

[88] P. Losada-Pérez, G. Pérez-Sánchez, C. Cerdeiriña, and J. Thoen, "Dielectric constant of fluids and fluid mixtures at criticality," Phys. Rev. E **81**, 041121 (2010).

[89] K. G. Wilson and M. E. Fisher, "Critical exponents in 3.99 dimensions," Phys. Rev. Lett. **28**, 240 (1972).

[90] C. Bervillier, "Universal relations among critical amplitude. Calculations up to order ϵ^2 for systems with continuous symmetry," Phys. Rev. Lett. **14**, 4964 (1976).